

PREDICTING PASSIVE INTESTINAL DRUG ABSORPTION: AN INTERESTING
RELATIONSHIP BETWEEN FRACTION ABSORBED AND MELTING POINT

by

Katherine A. Chu

A Dissertation Submitted to the Faculty of the
DEPARTMENT OF PHARMACEUTICAL SCIENCES

In Partial Fulfillment of the Requirements
For the Degree of

DOCTOR OF PHILOSOPHY

In the Graduate College

THE UNIVERSITY OF ARIZONA

2009

THE UNIVERSITY OF ARIZONA
GRADUATE COLLEGE

As members of the Dissertation Committee, we certify that we have read the dissertation prepared by Katherine A. Chu entitled Predicting Passive Intestinal Drug Absorption: An Interesting Relationship between Fraction Absorbed and Melting Point and recommend that it be accepted as fulfilling the dissertation requirement for the Degree of Doctor of Philosophy

_____ Date: November 25, 2009
Dr. Samuel H. Yalkowsky

_____ Date: November 25, 2009
Dr. Paul B. Myrdal

_____ Date: November 25, 2009
Dr. Michael Mayersohn

Final approval and acceptance of this dissertation is contingent upon the candidate's submission of the final copies of the dissertation to the Graduate College.

I hereby certify that I have read this dissertation prepared under my direction and recommend that it be accepted as fulfilling the dissertation requirement.

_____ Date: November 25, 2009
Dissertation Director: Dr. Samuel H. Yalkowsky

STATEMENT BY AUTHOR

This dissertation has been submitted in partial fulfillment of requirements for an advanced degree at the University of Arizona and is deposited in the University Library to be made available to borrowers under rules of the Library.

Brief quotations from this dissertation are allowable without special permission, provided that accurate acknowledgment of source is made. Requests for permission for extended quotation from or reproduction of this manuscript in whole or in part may be granted by the head of the major department or the Dean of the Graduate College when in his or her judgment the proposed use of the material is in the interests of scholarship. In all other instances, however, permission must be obtained from the author.

SIGNED: Katherine A. Chu

ACKNOWLEDGEMENTS

Thank you to Dr. Samuel H. Yalkowsky, my graduate advisor. I admire and respect his love for science, and his passion for teaching was clear every time we spoke. Dr. Y is a one-of-a-kind mentor who tailors his approach to each student individually. He takes into account students' personalities, including strengths, weaknesses and desired areas of research and learning. I'm forever indebted. Your wisdom and insight was truly a guiding force.

I would also like to acknowledge Dr. Michael Mayersohn, Dr. Paul Myrdal, Dr. Indraneel Ghosh, and Dr. Srinu Raghavan, my doctoral committee members. Thank you for your support and guidance. I would not be the scientist I am without your help.

Lastly, but certainly not least, I owe part of this achievement to my family and my dearest friends. Your deep love, support and encouragement propelled me through this challenging chapter of my life. Most importantly, I thank God for giving me the strength and peace-of-mind to become a Doctor.

DEDICATION

To Joe

TABLE OF CONTENTS

LIST OF FIGURES	10
LIST OF TABLES	11
ABSTRACT	12
CHAPTER 1: INTRODUCTION	13
1.1 Physicochemical and Physiological Factors That Affect Oral Drug Absorption ...	15
1.2 Physicochemical Parameters Used In <i>In Silico</i> Modeling	19
1.2.1 Lipophilicity.....	20
1.2.1.1 Molecular Size	21
1.2.1.2 Hydrogen Bonding.....	21
1.2.1.3 Polar Surface Area	21
1.2.2 Solubility.....	22
1.2.2.1 Log K_{ow}	22
1.2.2.2 Crystallinity.....	23
1.2.2.3 Ionization State	24
CHAPTER 2: COMPUTATIONAL MODELS TO PREDICT CACO-2 CELL MONOLAYER PERMEABILITY.....	26
2.1 Caco-2 Cell Monolayers	26
2.2 Molecular Descriptors.....	26
2.2.1 Log P and Log D.....	27
2.2.2 Charge	27

TABLE OF CONTENTS - *continued*

2.2.3 Molecular Weight	30
2.2.4 Hydrogen Bonding.....	31
2.2.5 Polar Surface Area	31
2.3 Conclusion	33
CHAPTER 3: COMPUTATIONAL MODELS TO PREDICT HUMAN PASSIVE	
INTESTINAL ABSORPTION	34
3.1 Molecular Descriptors.....	34
3.2 Lipinski's "Rule of Five".....	35
3.3 Theory of Mass Transport.....	36
3.4 Absorption Potential	37
3.5 pH-Independent Transport of Ionizable Drugs.....	38
3.6 Maximum Absorbable Dose	40
3.7 Modified Absorption Potential	42
3.8 Melting Point-Based Absorption Potential.....	45
3.9 Absorption Potentials Combined.....	49
3.10 Conclusion	61
CHAPTER 4: AN INTERESTING RELATIONSHIP BETWEEN DRUG	
ABSORPTION AND MELTING POINT	62
4.1 Introduction.....	62
4.1.1 Absorption Potential	64
4.1.2 Effect of pH on Transport for Saturated Solutions	64

TABLE OF CONTENTS - *continued*

4.1.3 Modified Absorption Potential	67
4.2 Methods	68
4.2.1 Compound Selection	68
4.2.1.1 Absorption Data	69
4.2.1.2 Physical Data	69
4.3 Results & Discussion	74
4.3.1 Modified Absorption Potential for Saturated Compounds (MAP)	74
4.3.2 General Solubility Equation.....	78
4.3.3 Melting Point-Based Absorption Potential (MPbAP)	79
4.3.4 Melting Point, Dose and Fraction Absorbed.....	81
4.4 Conclusion	85
CHAPTER 5: PREDICTING AQUEOUS SOLUBILITY: The Role of Crystallinity.....	87
5.1 Introduction.....	87
5.2 Method	88
5.3 Results & Discussion	89
5.4 Conclusion	98
CHAPTER 6: PREFORMULATION STUDY OF	
3-[(4-BENZYLPIPERAZINO)METHYL]-1H-INDOLE (UA8967).....	100
6.1 Introduction.....	100
6.2 Methods	101
6.2.1 Reagents.....	101

TABLE OF CONTENTS - *continued*

6.2.2 Apparatus	101
6.2.3 pH-Solubility and Stability Determination	102
6.2.4 Equilibrium Cyclodextrin Solubility and Stability Determination	103
6.2.5 Supersaturated Solution Preparation and Stability	103
6.3 Results.....	104
6.3.1 pH-Solubility.....	104
6.3.2 pH-Stability in Aqueous and Cyclodextrin Solutions.....	105
6.3.3 Cyclodextrin Solubility.....	108
6.3.4 Supersaturated Formulations	109
6.4 Discussion.....	111
6.4.1 Physicochemical Properties	111
6.4.2 Cosolvent Solubilization.....	111
6.4.3 pH-Solubility and Stability	111
6.4.4 Cyclodextrin Solubilization and Stabilization	112
6.4.5 Clear and Stable Supersaturated Solutions	114
6.5 Conclusion	115
REFERENCES	117

LIST OF FIGURES

Figure 2.1: Caco-2 cell permeability as a function of pH for alfentanil.....	29
Figure 3.1: Theoretical plot of the flux through Caco-2 cell monolayers as a function of pH for alfentanil in a hypothetical saturated solution.....	39
Figure 3.2: Relationship between the absorption potential parameter (AP_{Balon} and MAP) and fraction absorbed.....	50
Figure 4.1: Relationship between MAP and Fraction Absorbed.....	75
Figure 4.2: Relationship between $S_w^{int} \cdot K_{ow}$, Dose and Fraction Absorbed.....	77
Figure 4.3. Relationship between MPbAP and Fraction Absorbed.....	80
Figure 4.4: Relationship between Melting Point, Dose and Fraction Absorbed	82
Figure 6.1: pH-Solubility profile of UA8967	105
Figure 6.2: pH-stability data in aqueous and 40% cyclodextrin solutions at pH 3.....	107
Figure 6.3: pH-stability data in aqueous and 40% cyclodextrin solutions at pH 7.....	108
Figure 6.4: Solubility of UA8967 as a function of cyclodextrin concentration in phosphate buffer saline, pH ~ 7.6.	109
Figure 6.5: Equilibrium and supersaturated solutions of UA8967 in 20% cyclodextrin PBS solutions at 25°C and 5°C.....	110

LIST OF TABLES

Table 3.1. Calculated Maximum Absorbable Dose (MAD, mg) Based on Low, Medium and High Permeability and Solubility Values.....	41
Table 3.2. Interrelationship of Solubility, Partition Coefficient, Melting Point, and Dose for at Least 50% Absorption.....	47
Table 3.3 Physical Properties, Dose and Human Intestinal Absorption Data for Soluble Drugs.....	51
Table 3.4 Physical Properties, Dose, and Human Intestinal Absorption Data for Saturated Drugs.....	57
Table 4.1 Physical Properties, Dose and Human Intestinal Absorption Data.....	70
Table 4.2 Interrelationship of Solubility, Partition Coefficient, Melting Point, and Dose for at Least 50% Absorption.....	84
Table 5.1 Properties and Solubility Predictions of Compounds Studied by Box and Comer.....	92
Table 6.1. Experimental Intrinsic Aqueous Solubility, Solubility Product, and Dissociation Constants of UA8967.....	104
Table 6.2. pH Stability of UA8967 in Buffer Solutions With and Without Cyclodextrins at 25°C and 5°C	106

ABSTRACT

Oral drug administration remains the most popular route of drug delivery. Absorption of the dissolved drug through the intestinal epithelial membrane is a prerequisite to systemic bioavailability and drug efficacy. In efforts to reduce the long lead times, attrition rates, and costs of drug discovery and development, computational models have been developed to predict the membrane permeability and absorption efficiency of a dosed drug. Many models utilize various molecular descriptors to correlate with *in vitro* permeability or human intestinal absorption data. It is widely accepted that the two most significant physicochemical properties that control a compound's passive transport process are its aqueous solubility and lipophilicity characteristics.

This work will discuss the theoretical background of passive transport, a number of computational models developed to predict *in vitro* permeability, other models that predict human fraction of dose absorbed, and predicting absorption efficiency relative to a maximum dose. A newly developed prediction method is also presented, that reveals an interesting relationship between fraction absorbed and the melting point of the drug.

CHAPTER 1: INTRODUCTION

Many pharmaceutical companies are rethinking their approach to drug discovery research in response to the increasing costs of development (nearly \$1 billion dollars per marketed drug).^{1,2} Drug delivery and development practices are being integrated much earlier in the discovery process. Companies recognize that physicochemical and pharmacokinetic properties need to be addressed early in drug discovery to increase the chances of a creating a successful pharmaceutical product. The major reasons for the rising costs are high attrition rates, mainly due to poor pharmacokinetics/oral bioavailability, efficacy, and toxicity.³ According to Oprea,⁴ approximately one in a million compounds will likely reach the market. Efforts to improve the rational design of lead candidates and thereby streamline the drug discovery and development process should help to sustain a competitive industry.

A pharmaceutically successful therapeutic agent ideally should have high affinity and selectivity for its intended biological target, be orally bioavailable, cause minimal toxic or adverse reactions, and have elimination characteristics so as to provide a convenient dosing regimen (e.g., once a day). While combinatorial chemistry and high-throughput screening have produced thousands of hit-to-lead compounds with greater specificity towards biological targets, numerous fast and convenient computational models, based on structural and physicochemical properties, have already been devised to predict intestinal drug permeability and oral drug absorption. Various medium and high-throughput *in vitro*

absorption, distribution, metabolism, and excretion (ADME) screens have subsequently been developed to keep up with the high demands for large quantities of preliminary information. Compound toxicity screens have been developed to a lesser extent. The large amount of *in vitro* data being generated will be very useful for further developing computational models to predict ADME properties and ultimately serve to help reduce the risk of late-stage attrition.

As oral delivery remains the major route of drug administration, the focus of many computational models has been on predicting intestinal absorption since it is a necessary first step to bioavailability. These models range from simple to complex and they are developed based on any number of structural, physicochemical or physiological variables. The numerous models proposed can be broadly classified as *in vivo*, *in situ*, *in vitro*, and *in silico*, in order of biological relevancy. The following review will only focus on *in silico* models developed for predicting passive absorption. For more detailed discussions on predictive models of other ADME properties of interest, the reader is directed to a number of recent papers.⁵⁻⁹

The advantage of using *in silico* models in drug design and early drug discovery is that they completely avoid the use of animals and active experimentation. They require minimal time and labor since most physical property data upon which they are based, can be easily and quickly calculated directly from the chemical structure, and can be incorporated into theoretical and/or empirical models. Computational methods also have

the advantage that they can be applied to the design of chemical entities prior to synthesis. The resulting models along with other *in silico* models that provide more specific information on solubility and dose, can also aid in the selection of candidates for clinical development.

1.1 Physicochemical and Physiological Factors That Affect Oral Drug Absorption

A number of physicochemical and physiological factors affect oral drug absorption. The major determinants of passive absorption are drug solubility, dissolution rate, permeability, pK_a , and GI fluid pH. Other factors such as GI fluid volume, gastric emptying time, formulation, food composition, bile salts, specialized membrane transporters and metabolizing enzymes also affect absorption.

The extremely large surface area of the small intestine is the major site of oral drug absorption. A drug molecule must have the requisite membrane/water or oil/water partition characteristics in order to have adequate permeability. About 90% of marketed (in the USA) oral drugs have $\log K_{ow}$ values less than 5.5.¹⁰ Lipinski *et al.*¹¹ and Sakaeda *et al.*¹² observed that drugs having $\log K_{ow}$ values greater than 5 are likely to be poorly absorbed. The most likely reason for that isn't the inability of the solute to penetrate the intestinal membrane, rather, it is the lack of solute molecules present in solution. While lipophilicity promotes membrane permeability, it is unfavorable towards aqueous solubility. If the drug molecule is not available in solution, it cannot be absorbed through

the intestinal membrane. Not only does the solid drug need to be dissolved, but the degree of ionization is also an important factor in membrane transport, as the uncharged species is the predominant form to diffuse through the lipid bilayers. Hence, a drug's pK_a and the pH of the GIT are also important factors.

The dramatic changes in pH of the gastrointestinal tract play a significant role in the solubility and dissolution rate of ionizable drugs. In particular, ionization helps to increase the dissolution rate of poorly water-soluble compounds. The average pH values in healthy humans in the fasted state in the stomach, duodenum (mid-distal), jejunum, and ileum have been reported to be 1.3, 6.5, 6.6, and 7.4, respectively.¹³ Consequently, weak acids have lower solubility in the stomach and upon entering the upper small intestine, their solubility increases due to ionization. The converse is true for weak bases.

The dissolution rate of insoluble drugs is typically the major limitation to good absorption. A useful definition, as suggested by Horter and Dressman,¹³ for a poorly soluble drug is one for which the dissolution rate is longer than the transit time through its absorptive sites. The key factors to the kinetics of drug dissolution are described by the Noyes-Whitney equation:

$$DR = \frac{dM}{dt} = kA(C_s - C) \quad (1)$$

where DR is the dissolution rate, M is the mass of solute dissolved in time t , k is a constant that is related to the hydrodynamics of the dissolution medium, A is the surface area of the solute available for dissolution, C_s is the saturation solubility of the solute, and C is the bulk concentration of the solute in the medium. When the bulk concentration is considerably less than the drug's solubility, the system can be approximated by sink conditions, in which the concentration C in Equation 1 is assumed to be negligible. In this case, the dissolution rate is directly proportional to the solute's solubility. The greater the aqueous solubility, the greater the driving force for dissolution.

Particle size reduction, through milling, micronizing, microcrystallization, or grinding, is often employed to increase the surface area of the exposed solid drug. Given the higher energy state of the molecules at the surface, increases in the apparent solubility as well as the dissolution rate are observed. In addition, crystal form, polymorphs, amorphs, and hydrates/solvates can affect the apparent solubility and dissolution rate of drugs.

Formulations developed using metastable solid forms or as pharmaceutical salts may lead to supersaturation upon oral administration. The rapidly dissolving salt forms will be supersaturated with respect to the free acid or free base. The high energy metastable formulations will be supersaturated with respect to its true thermodynamic aqueous solubility. If the supersaturated solutions remain stable for as long as the small intestinal transit time, intestinal absorption should be improved. However, the potential for the

interconversion of the metastable form to the thermodynamically more stable form can be a limiting factor.

The rate and extent of drug absorption can also depend on fasted or fed conditions. The effect of food may cause delayed, decreased, increased, or no effect on drug absorption. The presence of solid foods, especially those with a high fat content, increases the gastric residence time. This may have several effects depending on the drug or dosage form ingested. Drugs that are predominantly absorbed in the small intestines will experience a decrease in the absorption rate because of the delay in gastric emptying. A delay in absorption will also occur for enteric coated drugs due to the delay in drug transit. For-pH sensitive chemically labile drugs, absorption may decrease due to the drug's prolonged residence time in the gastric fluids. For poorly soluble or dissolution rate-limited drugs, the more time the drug spends in the stomach, the more time it has to dissolve and that may allow absorption to be more complete. Drugs administered in solution or in a dispersed formulation will be less affected by food than those administered as a compressed tablet.¹⁴

Metabolizing enzymes and influx and efflux transporters are known to be expressed in the gut wall.¹⁵⁻¹⁸ Their interplay act to modulate intestinal drug absorption. Even at levels that are 50% of the hepatic level, the gut wall isozyme cytochrome P-450 3A4 (CYP3A4) can exert a considerable effect on the absorption of a compound, especially when the compound is also a substrate for the efflux transporter, P-glycoprotein (P-gp). The efflux

transporter recycles the drug from the enterocyte back into the gut lumen, allowing CYP3A4 a greater opportunity to metabolize the drug in the gut.^{16, 19} Other transport proteins help substrates get across the intestinal membrane. Active absorptive influx of compounds such as amino acids, oligopeptides, monosaccharides, mono- and dicarboxylic acids, bile acids, and several water-soluble vitamins, are also important in drug absorption.

As one can conclude, intestinal drug absorption is a complicated and intricate process involving numerous factors. While still affected by many of the above factors, passive diffusion of drug molecules, on the other hand, is a process that is much better understood. The ability to control the physicochemical properties of a compound that affect passive intestinal absorption would contribute significantly to the discovery and development of a successful therapeutic agent.

1.2 Physicochemical Parameters Used In *In Silico* Modeling

Medicinal chemists can design compounds to have the desired physicochemical properties for improved absorption. Various computational models have been constructed using structure-property or structure-activity relationships to predict passive intestinal drug absorption. They range from simple and intuitively easy to understand models that rely on rapid (on the order of milliseconds) counting of atoms or fragments to complex and time-consuming (on the order of minutes to weeks) methods involving molecular or

quantum mechanical calculations.²⁰ The two most fundamental physicochemical parameters of passive transport are lipophilicity and solubility. These are described below.

1.2.1 Lipophilicity

The lipophilic nature of a compound is crucial in determining how well the molecule can penetrate epithelial membranes which are lipid-like in character. Lipophilicity is a measure of polarity, or hydrophobicity, and is often expressed as a ratio of the compound's concentration in an oil phase to that in an equilibrated aqueous phase. By far, the most well accepted lipophilicity measurement is the octanol/water partition coefficient, K_{ow} , which is valid for uncharged species. For ionizable compounds, a distribution coefficient, which is dependent on pH and the compound's dissociation constant, is used to describe the lipophilic character of the charged species. It is the ratio of the total concentrations (*i.e.* the sum of the concentrations of the unionized and ionized forms) of the drug in the octanol phase to that in the aqueous phase.

Among the molecular descriptors that have been correlated with permeability or gastrointestinal absorption, some have been identified as components of lipophilicity, including molecular size, hydrogen bonding, and polar molecular surface area.

1.2.1.1 Molecular Size

Many different molecular size descriptors exist including van der Waals volume, molar volume, surface area, and molecular weight, MW. Based on correlation studies between volume and surface area to molecular weight,²¹ it is reasonable to use MW as a molecular size descriptor especially since it is easy to calculate. In a homologous series, volume or molecular weight is linearly correlated with $\log K_{ow}$.

1.2.1.2 Hydrogen Bonding

Hydrogen bonding strengthens intermolecular interactions through the sharing of the electrons of a hydrogen atom by two highly electronegative atoms, like nitrogen, oxygen, or fluorine. A hydrogen atom formally bonded to an electronegative atom is a hydrogen bond donor. An electronegative atom is a hydrogen bond acceptor regardless if it has hydrogen bonded to it or not. Typical measures of hydrogen bonding include the bond type, bond strength or the bond count, as in the number of H-bond donors or acceptors, or total number of H-bonds. The number of H-bond donors and acceptors is a measure of a solute's polarity, hence, it is also a measure of a solute's lipophilicity.

1.2.1.3 Polar Surface Area

The polar surface area, PSA, is defined as the area of the van der Waals surface occupied by nitrogen and oxygen atoms and their attached hydrogen atoms. Hence, PSA is another measure of a compounds capacity to form hydrogen bonds. PSA calculations can be based on a single conformation of the molecule or based on a Boltzmann-weighted

average of the surface area of each low-energy conformation by its probability of existence. The latter method is termed dynamic polar surface area, PSA_d .

1.2.2 Solubility

Aqueous solubility has long been recognized as a key physicochemical factor in controlling passive transport processes. It is the determining property that affects the dissolution rate of solid solutes. If a compound exhibits poor water solubility, very little solute will be available in solution for membrane permeation, most likely leading to poor drug efficacy. The intrinsic aqueous solubility of a compound refers to an equilibrium concentration of the unionized form in a saturated solution.

1.2.2.1 Log K_{ow}

As discussed previously, while $\log K_{ow}$ or lipophilicity, is one of the major determinants of membrane permeability, it is also an important component of aqueous solubility. Log K_{ow} and/or group contribution approaches have been the most common methods of estimating solubility. In general, there is an inverse relationship between solubility and partition coefficient, especially for liquid solutes. Hansch *et al.*²² showed that for a large number of organic liquids, the aqueous solubility can be accurately predicted based on $\log K_{ow}$ alone, by

$$\log S = A \log K_{ow} + B \quad (2)$$

where A and B are constants that depend on the data set considered. $\log K_{ow}$ has been used to reflect a compound's aqueous activity coefficient and represents the difference between the adhesive and cohesive interactions of water and solute. Yalkowsky²³ showed that the molar solubility of a liquid solute in water, S_w , can be described by

$$\log S_w = 0.5 - \log K_{ow} \quad (3)$$

1.2.2.2 Crystallinity

Not only does the aqueous solubility of a solid drug depend on how strongly the molecule associates with water (*i.e.*, aqueous activity), but an additional thermodynamic factor must be considered. The aqueous solubility of crystalline solutes is additionally governed by the intermolecular interactions associated with the crystal lattice. Strong crystal lattice interactions require more energy to separate the molecules from one another, leading to lower solubility. The melting point of a compound has been used quite commonly to reflect the strength of the crystal lattice. Therefore, strong crystal lattice interactions have higher melting temperatures than crystalline solutes that aren't as tightly bound to one another. Yalkowsky²³ showed that the role of drug crystallinity in determining solubility can be approximated by.

$$\log \frac{S^C}{S^L} = -0.01(MP - 25) \quad (4)$$

where S^C and S^L are the molar solubilities of the crystalline drug and its hypothetical liquid form, respectively, and MP is the Celsius melting point of the solute. Combining equations 3 and 4 gives the general solubility equation (GSE) of Jain and Yalkowsky²⁴:

$$\log S_w = 0.5 - \log K_{ow} - 0.01(MP - 25) \quad (5)$$

Note that for liquids the last term is set equal to zero.

The GSE is a simple equation that is semi-empirically derived from thermodynamic principles used to estimate the aqueous solubility of organic nonelectrolytes. It combines the roles of aqueous activity coefficient, as reflected by the octanol-water partition coefficient, and crystallinity, as reflected by the melting point term.

1.2.2.3 Ionization State

The pH of the aqueous environment can easily change the solubility of weak electrolytes. Weak acids are more soluble under higher pH conditions, such as in the small intestine, and weak bases are more soluble under lower pH conditions, such as in the stomach. Ionization can significantly improve the dissolution rate and total solubility of poorly soluble ionizable compounds. The fraction of the soluble drug in its unionized or ionized form depends on the pH of the environment and the drug's dissociation constant, pK_a . The fraction unionized for a weak acid is:

$$f_u = \frac{[HA]}{[HA] + [A^-]} \quad (6)$$

Where f_u is the fraction unionized, $[HA]$ is the concentration of the unionized species, and $[A^-]$ is the concentration of the ionized species. The concentrations of the unionized and ionized forms of an acidic drug are related by the Henderson-Hasselbalch equation.

$$\log \frac{[A^-]}{[HA]} = pH - pK_a \quad (7)$$

or

$$\log[A^-] = \log[HA] + pH - pK_a \quad (8)$$

This can be combined with the GSE (Equation 5) to determine the total solubility at any given pH.

$$S_{total} = S_w \cdot (1 + 10^{pH - pK_a}) \quad (9)$$

CHAPTER 2: COMPUTATIONAL MODELS TO PREDICT CACO-2 CELL MONOLAYER PERMEABILITY

2.1 Caco-2 Cell Monolayers

An *in vitro* surrogate membrane was developed to model the human small intestinal epithelium and to study drug transport. A monolayer of a human colon adenocarcinoma (Caco-2) cells are grown on a semi-permeable filters. Permeability measurements are made as the drug passively diffuses from a donor compartment to a receptor compartment. An advantage of the model is that the cell lines also express various biological membrane properties, including enzymatic and transporter proteins.¹ However, the predictive power of the model may be limited by the over-expression of P-glycoprotein in the cell line. Some researchers have overcome that complicating factor by adding known efflux inhibitors such as verapamil to the donor solution.²

2.2 Molecular Descriptors

Numerous studies report strong correlations of various molecular descriptors with Caco-2 cell monolayer permeability. Among the multitude of descriptors, the predominant properties shown to have strong correlations with Caco-2 permeability include lipophilicity, hydrogen bonding, size, polar surface area, and charge.¹⁻⁸ However, many

descriptors are interrelated and lead to some redundancies. It has been suggested that simple to calculate, one-dimensional molecular properties such as molecular weight and H-bonding descriptors, are the major components of lipophilicity and permeability, while charge can be accounted for in lipophilicity when the distribution coefficient is used.^{1,7} It is generally assumed that polar surface area is closely related to hydrogen bonding potential.^{6,8}

2.2.1 Log P and Log D

Calculations of partition coefficients or distribution coefficients are readily available from a variety of software programs, such as Biobyte⁹ and ACD Inc.¹⁰ Caco-2 cell permeability studies have shown a sigmoidal relationship between permeability and log partition coefficient, log K_{ow} or log distribution coefficient, log D.^{1,5,11} For ionizable solutes, it is important to take into consideration the relative fractions of the unionized and ionized species in solution, as it is generally accepted that the uncharged species is the predominant form to penetrate the lipid membrane.

2.2.2 Charge

This common assumption was confirmed in a study by Palm *et al.*² where they clearly show that total drug transport as a function of pH is strongly dependent on the available unionized fraction, f_u , and much less so on the ionized form, even when it exists at much higher concentrations. They studied the pH-dependent transport of two model cationic drugs, where one drug (alfentanil) is rapidly transported and the other drug (cimetidine) is

slowly transported across Caco-2 cell cultures. The pK_a values of alfentanil and cimetidine are very similar (6.5 and 6.8, respectively) while their $\log K_{ow}$ values differ significantly (2.16 and 0.40, respectively). Cell monolayer permeabilities were measured at various pH values (5.0-8.0). For alfentanil, the total permeability measured at pH 5.0 is 11.8×10^{-6} cm/s and increased to 327×10^{-6} cm/s at pH 8.0. By plotting the permeability as a function of f_u , Palm *et al.* obtained the following linear relationship (equation 9 in their paper):

$$P_c = 2.10 + 321 \cdot f_u \quad (1)$$

The slope of Equation 1 is taken to be the permeability coefficient of the unionized form, $P_{c,u}$, and the intercept is taken to be the permeability of the ionized form, $P_{c,i}$. The permeability coefficients for the unionized and ionized forms are 323×10^{-6} cm/s and 2.10×10^{-6} cm/s, respectively.² The experimental permeability data as a function of pH for alfentanil is plotted in Figure 2.1. The total permeability as a function of f_u is calculated by:

$$P_c = f_u \cdot P_{c,u} + (1 - f_u) \cdot P_{c,i} \quad (2)$$

The permeability of the ionized and unionized species are represented by the filled and open circles, respectively, and the solid curve is their sum, or the total permeability.

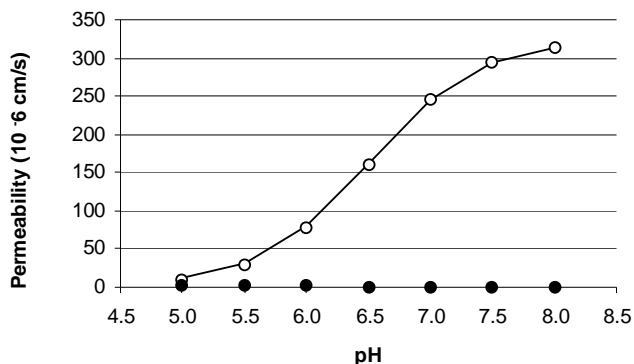


Figure 2.1. Caco-2 cell permeability as a function of pH for alfentanil. Permeability coefficients were obtained from Palm *et al.*² Filled circles (●) represent the permeability of the ionized species. Open circles (○) represent the permeability of the unionized species. The solid curve is the sum of the ionized and unionized permeabilities.

The results of this study by Palm *et al.*² show that total cell monolayer permeability decreases with a decrease in pH, as less of the favored uncharged form is available for transport. At low pH values for a basic drug, the small fraction of the uncharged solute, or the extremely low concentration available, greatly limits the total drug transport across the epithelial cells. This is observed in both the rapidly and slowly transported drug. For alfentanil, the fraction unionized at pH 5 is 0.031 while the fraction ionized is 0.969. It is only when f_u is much less than 0.1 that you see the greatest relative contribution of the ionized form, 17% (2.10×10^{-6} cm/s), to the total transport (11.8×10^{-6} cm/s). For the slowly transported drug cimetidine, the permeability of the ionized form at pH 5.0 (0.045×10^{-6} cm/s) contributed more than 60% to the overall transport (0.072×10^{-6} cm/s).²

2.2.3 Molecular Weight

While a single physicochemical parameter such as partition coefficient shows a strong correlation to permeability for a homologous series, weaker correlations with permeability are seen when structural diversity is introduced.¹² This suggests that other factors may be important in drug transport and should be incorporated into predictive models. Molecular weight and hydrogen bonding are two major components of lipophilicity. An interesting study by Camenisch *et al.*¹³ described the dependency of the Caco-2 cell permeability-lipophilicity relationship as a function of molecular weight. Different molecular weight ranges (MW < 200, MW 200-500, and MW > 500) gave different sigmoidal curves, with the smallest compounds lying to the left side of the plot, or lower log D values, and the largest compounds lying to the right, or towards higher log D values. It is suggested that the influence of molecular weight on the preferred transport pathway (*i.e.*, paracellular, transcellular, or endocytosis/transcytosis) leads to the shift in the permeability-lipophilicity relationship.

In plotting measured Caco-2 cell permeability values against the MW of seventeen drugs, it was clear that passive membrane transport is not simply correlated to molecular weight. Poor correlations are also obtained with other size descriptors when used alone.¹ As molecular weight and H-bonding descriptors have been shown to be two principal components of lipophilicity,^{1, 7, 13} when MW is combined with H-bonding factors, better correlations to Caco-2 permeabilities are observed.¹

2.2.4 Hydrogen Bonding

The hydrogen bonding potential is an important molecular surface property to consider in drug transport. Several reports suggest that properties associated with hydrogen bonding should be kept to a minimum to promote good permeability.^{3,4} Conradi *et al.*¹⁴ tested the hypothesis that compounds containing fewer hydrogen bonding sites should have improved permeability. They studied the influence of hydrogen bonding of peptides on the permeability across Caco-2 cell membrane in which the amide nitrogens were sequentially methylated. A strong correlation was observed between permeability and a decreasing number of hydrogen bonds. Conradi *et al.* suggest the mechanism to explain the improved permeability of the alkylated peptides could be due to the decrease in desolvation potential of the polar functional groups in the peptide. Since the sequential alkylation of the peptide did not result in substantial increases in $\log K_{ow}$, they concluded that the increase in flux did not appear to be correlated with lipophilicity.

2.2.5 Polar Surface Area

It is generally assumed that polar surface area is strongly correlated with hydrogen bonding potential. Based on principal component analysis, Stenberg *et al.*⁶ observed that the number rather than the strength of hydrogen bonding atoms contribute the greatest to polar surface area.

It is reasonable to expect that PSA will vary with conformation. Predicting intestinal permeability using single conformation or dynamic polar surface area calculations need to be considered carefully for larger and more flexible molecules, as intramolecular hydrogen bonding may be important for these compounds, and possibly lead to lower free energy changes involved in solute-solvent interactions that could have an effect on the permeability coefficient.

The use of a rapid, single-conformer-based calculation of PSA on a large range of compounds has been shown to give permeability predictions comparable to those obtained using dynamic PSA calculations.¹⁵ The work of Palm *et al.*⁵ reported a strong correlation between PSA_d and the permeability of Caco-2 cell monolayers of 6 beta blockers. In a later report, Palm *et al.*⁸ investigated the monolayer permeability to a series of 9 β -receptor-blocking agents using PSA_d in vacuum and in simulated chloroform and water environments. In general, good correlations between PSA_d and Caco-2 cell monolayer permeability were observed in all environments. They also showed the relationship between Caco-2 cell permeability and PSA_d was stronger than those between Caco-2 cell permeability and the calculated octanol/water distribution coefficients. Although good correlation was shown for this set of structurally similar compounds, using single molecular descriptors to predict cell membrane permeability may not be as good with drugs of greater structural diversity, as it was shown for a larger data set.¹⁵

2.3 Conclusion

Numerous studies attempt to correlate molecular descriptors with Caco-2 cell monolayer permeability, as it relates to intestinal absorption. In essence, these computational methods are “modeling” the model. Since the Caco-2 cell permeability technique, as well as other *in vitro* methods, require active experimentation with the synthesized compound of interest, it would be more efficient if computational techniques can be developed to reliably estimate ADME properties prior to compound synthesis. The development of such computational methods that relate structural and physicochemical properties to passive absorption are presented in Chapter 3.

CHAPTER 3: COMPUTATIONAL MODELS TO PREDICT HUMAN PASSIVE INTESTINAL ABSORPTION

3.1 Molecular Descriptors

The computational models described in Chapter 2 relate a compound's physicochemical properties to its Caco-2 cell permeability as an estimation of drug absorption. Several researchers have also examined solute descriptors directly against human intestinal absorption data. Palm *et al.*¹ observed a sigmoidal relationship between PSA_d and the human fraction of drug absorbed, FA. Among the twenty structurally diverse drugs in the data set, they observed that compounds that are completely absorbed ($FA > 0.90$) had a $PSA_d \leq 60 \text{ \AA}^2$ while drugs that are poorly absorbed ($FA < 0.10$) had a $PSA_d \geq 140 \text{ \AA}^2$. Clark² studied the same data set using the single conformational PSA calculation to predict FA. Similar results were obtained. However, when Clark applied the model to a larger data set (74 drugs), the correlation was not as good.

Zhao *et al.*³ used the general solvation equation developed by Abraham's group to model the human intestinal absorption data of 169 drugs. Of the five descriptors of the model, Zhao's evaluation showed that the most significant descriptors were the hydrogen bond acidity and basicity and volume, and that excess molar refraction and dipolarity/polarizability were not significant.

3.2 Lipinski's "Rule of Five"

A very popular guideline for the rapid profiling of compounds for improved absorption or permeability is Lipinski's⁴ "Rule of Five". The computational model is based on an analysis of 2245 drugs from the World Drug Index believed to have entered Phase II trials. The guideline is used to identify compounds that may possess poor absorption characteristics if any two of the following conditions are met:

Molecular weight > 500

Number of H-bond acceptors > 10

Number of H-bond donors > 5

Calculated log K_{ow} > 5.0

The "Rule of Five" has the advantage of not requiring any physical measurement of the drug, making it ideal for drug design. However, because of its empirical relationship based on the acceptance of drugs into phase II efficacy studies which does not always reflect passive absorption, its applicability to passive absorption is uncertain. Clearing phase I studies is not entirely due to satisfactory intestinal transport. Drugs that are poorly absorbed but effective and not toxic at very low blood concentration levels are likely to be selected for further study. Similarly, well absorbed drugs that are toxic will likely be discarded early.

Other computational methods developed to predict passive intestinal absorption use $\log K_{ow}$, solubility, melting point, and dose. In addition to a compound's permeability characteristics, the aqueous solubility must also be considered since the flux of a solute across the intestinal membrane is driven by its concentration gradient.

3.3 Theory of Mass Transport

Virtually all computational models developed to predict passive intestinal absorption are based on the theory of Stehle and Higuchi^{5,6} on the mass transport of a solute across a membrane by passive diffusion. In these models the transport rate, or flux F , is given by

$$F \propto \Delta C \cdot K_{mw} \quad (1)$$

where ΔC is the concentration gradient across the membrane and K_{mw} is the membrane-water partition coefficient. Equation 1 is applicable under steady-state conditions where the concentrations have no time dependence, that is, the concentration differential across the membrane is constant. Using silicone rubber membranes, Flynn and Yalkowsky⁷ and Flynn *et al.*⁸ showed that in the case of drug suspensions, the flux is given by

$$F \propto S_w^{int} \cdot K_{mw} \quad (2)$$

where S_w^{int} is the intrinsic molar solubility of the unionized form of the drug in water and K_{mw} is its membrane-water partition coefficient. Yalkowsky *et al.*^{9,10} then showed that

the above relationship can be applied to the transport of alkyl-p-aminobenzoates across the gills of goldfish by replacing the membrane-water partition coefficient with the octanol-water partition coefficient, K_{ow} .

3.4 Absorption Potential

A dimensionless parameter known as the absorption potential, AP, was derived by Dressman *et al.* in 1985¹¹ as a first approximation to predicting oral absorption:

$$AP = \log \left(K_{ow} \cdot F_u \cdot \frac{S_w^{int} \cdot V}{D} \right) \quad (3)$$

Their approach related the fraction absorbed to the octanol-water partition coefficient, K_{ow} , the intrinsic aqueous solubility, S_w^{int} , the fraction unionized, F_u , the dose administered, D , and the volume of the GI lumen, V . They observed a sigmoidal relationship between the AP and the human fraction of drug absorbed for the seven drugs studied.

While the S_w^{int} and F_u terms in Dressman's¹¹ absorption potential parameter account for the concentration of the unionized species at a pH 6.5, the K_{ow} term, as it's defined, only reflects the partition coefficient of the uncharged form. A more quantitative model was later introduced by Balon *et al.*¹² and is based on the solubility of the drug in water at pH 6.8, $S_T^{6.8}$, and the distribution coefficient at the same pH, $K_D^{6.8}$.

$$AP_{Balon} = \log\left(\frac{S_T^{6.8} \cdot K_D^{6.8} \cdot V}{D}\right) \quad (4)$$

Again, a sigmoidal relationship between the absorption potential of 20 drugs and their fraction of dose absorbed was observed.

3.5 pH-Independent Transport of Ionizable Drugs

The significance of including a term to account for the uncharged form is based on the generally accepted notion that it is the predominant species to penetrate the lipid membrane; whereas the permeation of the ionized form is considered negligible.

It is important to note that there are instances when drug transport is independent of pH.

When a saturated solution or suspension exists, the concentration of the uncharged species, or its intrinsic solubility, is constant across all pH values, even though its fraction may change with respect to pH. If the concentration of the unionized form is constant with pH, then so should the permeability profile.

A theoretical plot in Figure 3.1 illustrates the point just discussed, using alfentanil as an example. In instances where the drug concentration is less than its solubility, drug transport is pH-dependent as already illustrated in Figure 2.1. To convert the permeability data as a function of the unionized fraction, a drug concentration is needed. In the study by Palm *et al.*,¹³ they reported a concentration range of 0.5-10 mM. Assuming the

concentration of alfentanil is 1.0mM, multiplying f_u and $(1-f_u)$ by the concentration, times their respective permeability coefficients, would give the flux in units of mM·cm/s as a function pH. The profile would look identical to Figure 2.1. The total flux is calculated by:

$$P_{total} \cdot C_{total} = C_u \cdot P_{c,u} + C_i \cdot P_{c,i} \quad (5)$$

In contrast, when the drug concentration is at its solubility limit, such as in saturated solutions, permeability becomes nearly independent of pH, as the theoretical plot in Figure 3.1 shows. Here, the GSE was used to estimate alfentanil's intrinsic solubility of 1.5 mM based on a melting point of 141°C and a ClogP of 2.16. Equation 5 is used to calculate the flux for alfentanil with a solubility of 1.5mM and a $P_{c,u}$ and $P_{c,i}$ as reported by Palm *et al.*¹³

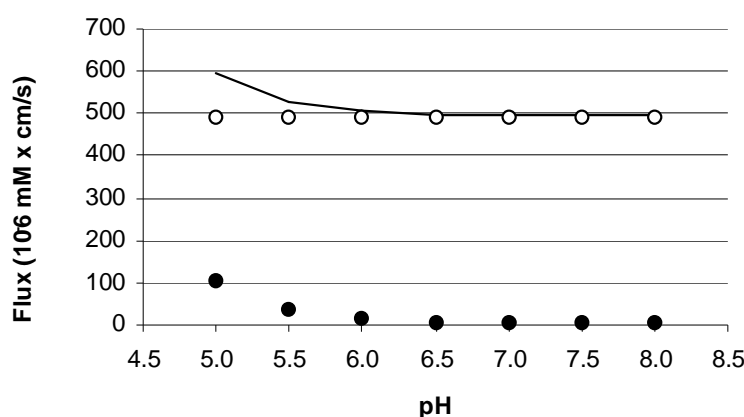


Figure 3.1. Theoretical plot of the flux through Caco-2 cell monolayers as a function of pH for alfentanil in a hypothetical saturated solution. The GSE was used to calculate alfentanil's solubility of 1.5mM. Permeability coefficients were obtained from Palm *et al.*¹³ Filled circles (●) represent the flux of the ionized species. Open circles (○) represent the flux of the unionized species. The solid curve is the total flux of the ionized and unionized form.

Whether the drug is at saturation (Figure 3.1) or below saturation (Figure 2.1), the overall permeability profile (solid curve) is largely dictated by the amount of the unionized species (open circles) in solution. The ionized form (filled circles) contributes negligibly to the total transport, except when f_u is very small (*i.e.*, at low pH values for a basic drug). Again, it is only when f_u is much less than 0.1 that the relative contribution of the ionized form is even noticeable at all.

3.6 Maximum Absorbable Dose

Johnson and Swindell¹⁴ introduced the concept of a maximum absorbable dose, MAD. They used a computational method to simulate the percent of dose absorbed as a function of solubility, absorption rate constant, k_a , the small intestinal water volume, and the small intestinal transit time, t .

$$MAD = k_a \cdot S_w^{\text{int}} \cdot V \cdot t \quad (6)$$

Johnson and Swindell note that their dissolution model was only validated on a relatively small set of neutral organic drug molecules. The hypothetical results indicate that above a given dose level where a saturated solution is maintained, discrete combinations of solubility and absorption rate constant yield a unique maximum absorbable dose,

regardless if higher doses are given. In fact, higher doses only resulted in a decrease in percent absorbed. For every 10-fold change in either the solubility value or the absorption rate constant, a corresponding 10-fold change is observed in the MAD. In other words, if the absorption rate constant is fixed, the maximum absorbable dose gets larger as the drug's solubility gets larger. Table 3.1 is an adapted version of Johnson and Swindell's¹⁴ model of the maximum absorbable dose for a hypothetical 200 Dalton drug dosed in 250 ml of water with a transit time of 6 hours. Low, medium and high absorption rate constants and solubility values were taken from their paper to calculate the maximum absorbable dose (mg)

Table 3.1. Calculated Maximum Absorbable Dose (MAD, mg) Based on Low, Medium and High Permeability and Solubility Values

Permeability (min^{-1})	Maximum Absorbable Dose (mg)			Solubility (M)
	0.01	0.1	1	
0.001	0.5	5	50	
0.01	5	50	500	
0.1	50	500	5000	

Intuitively, the model is easy to understand, but practically speaking, an absorption rate constant is not easily estimated from a compound's structure, thereby limiting its utility in early drug discovery. However, once an absorption rate constant is determined, the

model allows the team to check whether a compound has favorable absorption-related physicochemical properties or whether to expect pharmaceutical development challenges.

3.7 Modified Absorption Potential

Interestingly, an independent research group^{15,16} developed a modified absorption potential, MAP, model that demonstrates a similar concept to the MAD, but which is based on experimental human intestinal absorption data and uses lipophilicity and solubility as the key input parameters. The model's approach essentially uses solubility and $\log K_{ow}$ to determine if the drug will be well absorbed when given below a maximum dose level. The maximum dose can be determined from the product of the solubility and partition coefficient terms as described below. An advantage of their approach is that lipophilicity, or $\log K_{ow}$, can be reliably calculated from structure. A couple of disadvantages are that the model is only applicable to passive transport and that robust computational predictions of solubility are currently still lacking.¹⁷ However, if the melting point and $\log K_{ow}$ of a compound are known, the GSE can be used to give reasonably accurate solubility predictions.

Sanghvi *et al.*¹⁵ proposed a modified absorption potential, MAP, that requires only S_w^{int} and K_{ow} as physicochemical input parameters, instead of $S_T^{6,8}$ and $K_D^{6,8}$, as proposed by Balon *et al.*¹² The use of the terms S_w^{int} and K_{ow} provides an advantage since they are easier to measure and to calculate than S_T and K_D and consequently it is not necessary to

consider the pK_a of the drug. Furthermore, their use eliminates the potential inaccuracies of determining distribution coefficients and solubilities at a specific pH. It also avoids the inability of a single pH value to model the entire absorbing region of the small intestine. Assuming the volume of the GI lumen is 0.250 L, the MAP is expressed as:

$$MAP = \log\left(\frac{S_w^{int} \cdot K_{ow}}{4 \cdot Dose}\right) \quad (7)$$

The rationale to use the intrinsic properties rather than the solubility and distribution coefficient at a specific pH is based on a useful simplification described by Ni *et al.*¹⁸ Basically, the product of S_w^{int} and K_{ow} is equal to the product of S_T and K_D , for which both are constant over a wide pH range. This relationship is only valid when the given dose in 250ml of water is greater than the drug's intrinsic solubility. In other words, it only applies when the drug exists as a saturated solution, or a suspension, in the GI tract. For the combined 27 compounds analyzed by Dressman *et al.*¹¹ and Balon *et al.*,¹² Sanghvi reported that the fraction of drug absorbed is correlated as well as or better with MAP than with AP.

Based on the MAP model, Sanghvi *et al.*¹⁹ went on to develop another absorption parameter, π , where a single delineator was identified that was able to correctly classify 86 out of a set of 98 passively absorbed drugs to be either well absorbed or poorly absorbed. The absorption parameter includes a luminal oversaturation number, O_{LUMEN} ,

which was used to distinguish between high and low solubility drugs or drugs that existed as a solution or a suspension in the luminal volume. Unfortunately, the derivation of this new absorption parameter utilized the relationship of the products of $S_w^{int} \cdot K_{ow}$ and $S_T \cdot K_D$ expressed by Ni *et al.*,¹⁸ which is not applicable to subsaturated solutions. It should be noted, Sanghvi's π parameter was used by Yalkowsky *et al.*²⁰ in developing a 'rule of unity'.

From an initial data set of 219 structurally diverse compounds, only 91 drugs met the selection criteria for saturated (*i.e.*, dose in 0.250L > S_w^{int}) and passively absorbed drugs, which were evaluated by Chu and Yalkowsky¹⁶ using the MAP model. Based on the results, they were able to identify a single MAP delineator for the prediction of whether an orally administered drug at saturation will be well absorbed ($FA \geq 0.5$) or poorly absorbed ($FA < 0.5$). The model gave a prediction rate of 92%, where drugs with MAP values greater than 0 were at least 50% absorbed and drugs with MAP values less than 0 were less than 50% absorbed. The delineator establishes absorption efficiency and provides a simple means to estimate whether or not an orally administered drug undergoing passive transport will be absorbed efficiently. Based on the delineator of $MAP \geq 0$, a maximum dose for at least half of the dose to be absorbed can be calculated and is related to the drug's solubility and $\log K_{ow}$ value.

$$MAP = \log\left(\frac{S_w^{int} \cdot K_{ow}}{4 \cdot Dose}\right) \geq 0 \quad (\text{criteria for } FA \geq 0.5) \quad (8)$$

or

$$\log(S_w^{\text{int}} \cdot K_{ow}) \geq \log(4 \cdot Dose) \quad (9)$$

As long as the log of the product of solubility and partition coefficient is greater than the dose term, the drug should be well absorbed. Equation 9 allows one to quantitatively relate physicochemical parameters to drug transport, giving a maximum acceptable dose that achieves high absorption efficiency.

Johnson and Swindell's¹⁴ MAD and Sanghvi's MAP,¹⁵ both help expand our appreciation of the need for a solubility term relative to dose, along with lipophilicity, to better predict oral absorption. The simple and easy to calculate properties of the MAP model make it useful across all stages of discovery and development. However, a larger database that includes a substantially greater number of poorly absorbed compounds is needed to prove the existence of a clear delineator. Unfortunately, human absorption data for poorly soluble drugs that are poorly absorbed is sparsely published in the literature.

3.8 Melting Point-Based Absorption Potential

Another potentially useful absorption potential model was developed and takes advantage of the fact that the melting point of a compound is one of the first and more reliable physical properties measured. Chu and Yalkowsky¹⁶ introduced the melting point-based absorption potential, MPbAP, derived from Sanghvi's MAP and the General Solubility Equation²¹:

A rearranged GSE gives:

$$\log(S_w^{\text{int}} \cdot K_{ow}) = 0.5 - 0.01(MP - 25) \quad (10)$$

Replacing the log of the product of S_w^{int} and K_{ow} in Equation 7 with the right-hand side of equation 10 results in the melting point-based absorption potential, MPbAP:

$$MPbAP = 0.5 - 0.01(MP - 25) - \log(4 \cdot Dose) \quad (11)$$

The MPbAP model essentially collapses the two key physicochemical properties of passive intestinal absorption into a single, more easily measured property. While the convenience of the model allows the use of melting point to estimate fraction absorbed, fundamentally, the prediction, and therefore, passive transport, is still based on the key physicochemical properties of solubility and partition coefficient.

An absorption efficiency delineator has also been established in the MPbAP model using the same 91 compounds in the MAP model,¹⁶ giving 90% correct predictions of drugs being well absorbed and poorly absorbed based on their melting point. Drugs with MPbAP values ≥ 0 are expected to be well absorbed. In general, low melting compounds will be better absorbed than high melting compounds. It has been suggested that a compound with a high melting point ($> 250^\circ\text{C}$) which will be poorly soluble, may negatively impact oral absorption.²² Again, a maximum dose can be calculated based on the following relationship:

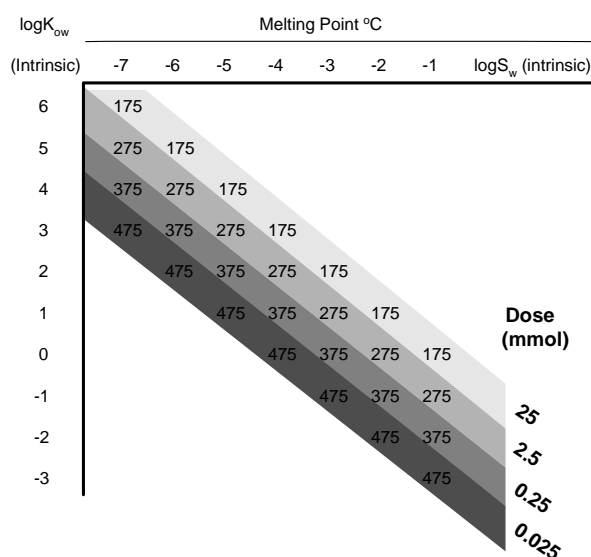
$$MPbAP = 0.5 - 0.01(MP - 25) - \log(4 \cdot Dose) \geq 0 \quad (12)$$

or

$$0.75 - 0.01MP \geq \log(4 \cdot Dose) \quad (13)$$

Table 3.2 illustrates the interdependencies of S_w^{int} , K_{ow} , melting point, and dose in determining FA. If the solubility and partition coefficient values, found along the horizontal and vertical axes, respectively, are known, then the corresponding melting temperature can be found in the table. Likewise, if the melting point of a drug is known, the product of S_w^{int} and K_{ow} is defined, and various combinations of solubility and partition coefficients can be determined. Combining Table 3.2 with dose levels completes the prediction of fraction absorbed.

Table 3.2. Interrelationship of solubility, partition coefficient, melting point, and dose for at least 50% absorption



An excellent review by Thomas *et al.*²² breaks down the pivotal physicochemical and pharmacokinetic parameters that contribute to poor oral bioavailability. They state that a minimal acceptable oral bioavailability of 30% has been set as a target within a typical oral drug development program. With this as a minimum threshold for the percent of oral dose absorbed, the MAP and MPbAP model can be a useful tool, particularly at the early stages of preclinical development (*i.e.*, at the beginning of the road map in Figure 3 of the article by Thomas *et al.*). As solubility, log P and melting point data are typically available early on, applying them in the MAP and MPbAP model allows the incorporation of dose information earlier into the decision making process. Estimations can be made to determine what the maximum dose is for a compound to be well absorbed. If the maximum dose is high (*e.g.*, milligram to gram scale), there is a higher confidence that the lead candidate will face less development challenges as it possesses more favorable solubility and lipophilicity characteristics for good absorption, and absorption efficiency is not as sensitive to dose. If the dose is low (*e.g.*, microgram to milligram scale), greater development efforts may be required to troubleshoot what factors are responsible for low absorption. Design of novel formulations may be necessary for these compounds in order to enhance its absorption profile, and absorption efficiency will be highly sensitive to dose amount. Furthermore, the pharmacokinetic profile of this type of compound will be very important to understand as intestinal or hepatic metabolism, for example, will result in even less of the dose absorbed and available to the systemic circulation.

The MAP and MPbAP models described above are valid only for saturated solutions, *i.e.*, for drugs that are less soluble than the dose in 0.250 L of water. Unfortunately, the data set used is heavily biased (87%) towards well-absorbed drugs. Only 12 of the 91 drugs studied are less than 50% absorbed.

3.9 Absorption Potentials Combined

If the model of Balon *et al.*¹² is applied to drugs that have doses that are soluble in 0.250 L of water and combined with the MAP model, the data set is increased to 249 compounds, 51 of which are poorly absorbed. Figure 3.2 illustrates this combination. The solubility and distribution coefficient values at pH 6.8 for each of the soluble drugs are calculated using ACD Inc.²³ A complete list of the 249 drugs and their experimental fraction absorbed data and their physical property data are provided in Table 3.3 (drugs that are soluble at the dose given in 250 ml) and Table 3.4 (drugs that are insoluble at the dose given in 250 ml). Figure 3.2 is divided into four quadrants by a horizontal line at 50% absorption and a solid vertical line at AP_{Balon} or $MAP = 0$. Approximately 81% of the drugs lie in the upper right and lower left quadrants, indicating that the delineator does a reasonable job at discriminating absorption efficiency.

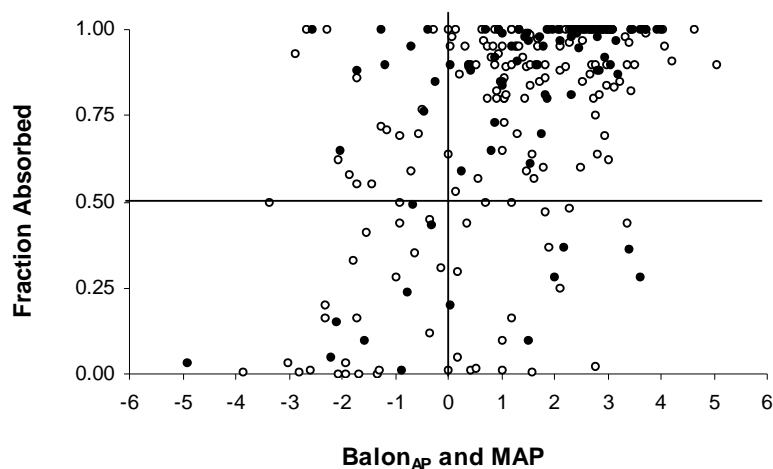


Figure 3.2. Relationship between the absorption potential parameter (AP_{Balon} and MAP) and fraction absorbed. AP_{Balon} is applied to high solubility drugs as represented by open circles (○). MAP is applied to solubility-limited drugs as represented by filled circles (●).

As with any model, the success of the AP_{Balon} or MAP models highly depend on the quality and accuracy of the data. Errors may come from any one or a combination of sources in: experimental or calculated solubility, calculated partition coefficient, dose, human absorption data, or simply from the failure of the model. A prediction rate of 81% is quite good in light of the different degrees of uncertainty for all of the measured and/or predicted data.

Table 3.3 Physical Properties, Dose and Human Intestinal Absorption Data for Drugs in Solution

Drug Name	FA	D(mg)	Reference for FA and Dose	MW	logS _T ^{6.8 f}	logD ^{6.8 f}
Acarbose	0.02	200	a	646	-0.83	-6.66 ^g
Acebutolol	0.80	300	a	336	-1.09	-0.29
Acetaminophen	0.80	700	b	151	-1.17	0.34
Acrivastine	0.88	8	b	348	-3.98	2.04
Acyclovir	0.20	350	c	225	-2.77	-1.76
Adefovir	0.16	210	a	273	0.87	-5.70
Albuterol	0.83	3	d	239	1.13	-2.32
Alendronate	0.01	5	b	249	4.55	-7.64
Alprazolam	0.90	1	a	309	-4.15	2.19 ^g
amikacin	0.00	400	b	586	-1.63	-4.12
Amiloride	0.50	20	c	214	-3.26	1.04
Aminopyrine	1.00	250	a	231	-1.91	0.75
Amoxicillin	0.93	688	a	365	-2.88	-2.12
Amphetamine	0.90	20	a	135	1.29	-1.01
Ampicillin	0.62	500	a	349	-2.86	-1.44
Amrinone	0.93	113	a	189	-1.15	-0.54
Antipyrine	0.97	700	a	188	-1.44	0.27
Ascorbic acid	0.35	1000	a	176	2.55	-4.81
Atenolol	0.50	200	a	266	0.37	-2.19
Atropine	0.98	2	a	289	0.10	-1.31
Azosemide	0.10	50	a	371	-3.47	1.21
Baclofen	0.95	15	d	214	-1.58	-0.94
Benazepril	0.37	20	a	425	-2.70	0.88
Benzylpenicillin	0.30	500	a	334	-0.07	-1.99
Betaxolol	0.90	20	a	307	-1.00	0.39
Bromazepam	0.84	6	a	316	-3.19	2.06
Bumetanide	0.96	0.5	a	364	-1.94	0.08
Caffeine	1.00	151	a	194	-1.73	-0.13
Capreomycin	0.50	100	a	653	0.68	-7.25

Drug Name	FA	D(mg)	Reference for FA and Dose	MW	logS_T^{6.8 f}	logD^{6.8 f}
Captopril	0.84	100	a	217	1.55	-2.74
Cefamandole Nafate	0.00	2000	b	462	-1.36	-2.09
Ceforanide	0.00	1000	b	520	-1.15	-2.90
Ceftizoxime	0.72	500	a	382	-0.65	-2.89
Ceftriaxone	0.01	400	a	554	-0.55	-4.57
Cefuroxime	0.01	1000	a	424	-0.17	-3.16
Cefuroxime axetil	0.44	500	a	510	-0.17	-3.16
Cephalexin	1.00	500	a	347	-2.42	-2.10
Chloramphenicol	0.90	250	a	323	-3.16	1.02
Cidofovir	0.03	700	a	279	2.03	-7.03
Cimetidine	0.64	200	a	252	-2.05	-0.45
Ciprofloxacin	0.69	200	a	331	-2.65	-0.87
Clonidine	0.95	0.3	a	230	-1.83	0.61
Codeine	0.95	70	a	299	-1.49	-0.26
Corticosterone	1.00	3.0	c	346	-3.43	1.76
Cromolyn	0.01	18.3	b	468	0.22	-2.45
Cycloserine	0.73	250	a	102	0.95	-1.89
Cymarine	0.47	3	a	548	-3.11	0.27
Dapsone	0.90	50	d	248	-2.85	0.94
Dexamethasone	0.80	1.5	a	392	-3.94	1.87
Digoxin	0.81	1.2	a	781	-3.23	0.85
Dihydrocodeine	0.89	60	a	301	-1.37	-0.24
Diltiazem	0.92	180	c	415	-2.91	1.54
Doxorubicin	0.12	55	a	543	-4.81	1.07
Eflornithine	0.55	1050	a	182	-0.86	-2.48
Enalapril	0.65	10 ^e	c	493	-2.51	-0.57
Enalaprilat	0.25	10	a	348	0.15	-1.99
Enoxacin	0.70	200	c	320	-2.92	-0.23
Ethambutol	0.80	1400	a	204	1.88	-2.71
Etoposide	0.50	350	a	588	-3.85	0.30
Famciclovir	0.77	313	a	321	-2.24	-0.67
Famotidine	0.45	40	b	337	-2.19	-1.50

Drug Name	FA	D(mg)	Reference for FA and Dose	MW	$\log S_T^{6.8 f}$	$\log D^{6.8 f}$
Felbamate	0.90	650	a	238	-2.73	1.19
Fenoterol	0.60	13	a	303	-0.11	-1.19
Fleroxacin	0.95	400	c	369	-3.30	0.96
Fluconazole	0.95	100	a	306	-3.06	0.50
Flumazenil	0.95	200	a	303	-3.11	1.08 ^g
Flunitrazepam	0.90	1	c	313	-3.45	1.25
Fluoxetine	1.00	30	c	309	-1.95	1.22
Fosfomycin	0.31	2100	a	138	5.33	-6.70
Gabapentin	0.59	500	a	171	-1.33	-1.31
Gallopamil	1.00	25	a	485	-2.88	1.49
Ganciclovir	0.03	75	a	255	-2.78	-2.07
Glibenclamid	1.00	3.1	c	476	-3.91	2.16
Hydrochlorothiazide	0.69	44	a	298	-1.15	0.88
Isoniazid	0.80	300	a	137	-0.12	-0.89
Kanamycin	0.01	4000	a	484	-1.53	-3.88 ^g
Ketorolac	0.90	10	a	255	-0.64	-0.41
K-strophanthoside	0.16	5	a	873	-1.87	-1.60
Lactulose	0.01	10000	a	342	-0.52	-3.21
Lamivudine	0.87	100	a	229	-1.83	-0.71
Levodopa	0.86	250	a	197	-1.27	-2.73
Lidocaine	1.00	153	c	234	-1.01	0.64
Lisinopril	0.28	15	a	405	-3.44	-1.38
Loracarbef	1.00	300	a	349	-1.26	-3.86
Lormetazepam	1.00	2	a	335	-4.23	2.36
Lornoxicam	1.00	4	a	372	-1.72	0.27
Mannitol	0.16	500	a	182	0.98	-4.67
Metaproterenol	0.44	1.6	a	211	1.03	-2.19
Metformin	0.53	1000	a	129	2.93	-4.31
Methotrexate	0.70	354	a	454	-3.28	-0.53 ^g
Methyldopa	0.41	250	a	211	-1.50	-2.38
Methylprednisolone	0.82	0.6	a	374	-3.75	1.99
Metolazone	0.64	2.5	a	366	-4.99	3.25

Drug Name	FA	D(mg)	Reference for FA and Dose	MW	logS _T ^{6.8 f}	logD ^{6.8 f}
Metoprolol	0.98	300	c	267	-0.17	-0.51
Metoprolol	0.95	300	a	267	-0.17	-0.51
Metronidazole	0.95	250	d	171	-1.38	-0.01
Morphine	0.85	20	a	285	-0.81	-1.04
Moxonidine	0.99	0.3	b	242	-0.87	-0.70
N-Acetylprocainamide	0.85	1.5	c	277	-0.01	-1.43
Nadolol	0.57	80	a	309	-0.35	-1.01
Naloxone	0.91	0.1	a	327	-2.87	1.18
Neomycin	0.01	2800	a	615	-1.45	-6.47 ^g
Nizatidine	0.90	150	a	331	-2.41	0.55
Norfloxacin	0.71	400	a	319	-2.75	-0.70
Olanzapine	0.75	10	b	312	-3.27	2.16
Ouabain	0.01	8	a	584	-2.10	-1.64
Oxazepam	0.89	15	a	287	-3.78	2.31
Oxprenolol	0.95	160	a	265	-0.51	0.00
Oxycodone	0.60	22.5	d	315	-2.56	0.81
Paracetamol	1.00	750	c	151	-1.17	0.34
Pefloxacin	1.00	500	c	333	-3.15	0.66
Pentazocine	1.00	50	c	285	-1.95	2.43
Pentobarbital	1.00	75	c	226	0.56	-1.32
Phenazone	0.99	450	b	188	-3.18	2.71
Phenobarbital	0.90	115	c	232	-2.53	1.64
Phenoxyethylpenicillin	0.59	22	a	350	-0.33	-1.78
Pindolol	0.92	1050	c	248	-0.61	-0.35
Pindolol	0.87	15	a	248	-0.61	-0.35
Piroximone	0.81	56	a	217	-1.42 ^h	0.96 ^g
Practolol	0.95	313	a	266	0.10	-1.69
Prazosin	0.86	1	a	383	-3.03	-0.12
Prednisolone	0.99	30	a	360	-3.45	1.49
Procainamide	1.00	4.5	c	235	0.55	-1.68
Progesterone	1.00	1.75	a	314	-4.67	4.04
Raffinose	0.00	8000	a	504	-1.76	-4.66 ^g

Drug Name	FA	D(mg)	Reference for FA and Dose	MW	logS _T ^{6.8 f}	logD ^{6.8 f}
Ranitidine	0.64	60	a	314	-1.18	-0.37
Ribavirin	0.33	800	a	244	-1.41	-2.26
Rimiterol	0.48	10	a	223	1.21	-2.69
Salicylic acid	1.00	300	c	138	1.45	-1.00
Scopolamine	0.90	0.010	c	303	-1.36	-0.47
Sorivudine	0.82	20	a	349	-1.93	-0.79
Stavudine	1.00	40	a	224	-1.11	-0.86
Sulfamethoxazole	1.00	800	d	253	-1.79	-0.10
Sulindac	0.90	200	a	356	-2.15	1.04
Sulpiride	0.44	200	a	341	-0.60	-1.67
Sultopride	0.89	75	a	354	-0.77	-1.22
Sumatriptan	0.57	200	a	295	-0.11	-1.88
Tenidap	0.89	120	a	321	-3.39	0.94
Tenoxicam	1.00	55	a	337	-1.08	-0.77
Terazosin	0.90	7.5	a	387	-2.45	-1.12
Terbutaline	0.62	5	a	225	0.79	-1.84
Theophylline	0.98	600	c	180	-1.62	-0.18
Timolol	0.95	30	a	316	-0.13	-1.95
Tobramycin	0.00	70	b	468	4.80	-9.37
Topiramate	0.86	650	a	339	-4.02	2.97
Torsemide	0.96	10	a	348	-3.27	1.60
Tranexamicacid	0.55	1250	a	157	-0.75	-2.19
Triamcinolone	1.00	0.3	d	394	-3.43	0.83
Trihexyphenidyl	1.00	2.5	c	302	-1.59	1.73
Trimethoprim	0.97	2	a	290	-2.29	0.25
Vigabatrin	0.58	2000	a	129	-0.48	-2.60
Xamoterol	0.05	125	a	339	0.25	-2.90
Zalcitabine	0.85	0.75	d	211	-1.02	-1.30
Zidovudine	1.00	700	a	267	-1.32	-0.53
Zopiclone	0.80	8	b	389	-3.09	0.45

^a Zhao *et al.*, 2001. Evaluation of human intestinal absorption data and subsequent derivation of a quantitative structure-activity relationship (QSAR) with the Abraham descriptors. *J. Pharm. Sci.*, 90, 749-784.

- ^b Sanghvi *et al.*, 2003. Predicting passive intestinal absorption using a single parameter. *QSAR Comb. Sci.*, 22, 247-257.
- ^c Willmann *et al.*, 2004. A physiological model for the estimation of the fraction dose absorbed in humans. *J. Med. Chem.*, 47, 4022-4031.
- ^d Hou *et al.*, 2007. ADME evaluation in drug discovery. 7. Prediction of oral absorption by correlation and classification. *J Chem Inf Model*, 47, 208-218.
- ^e Portoles *et al.* 2004. Bioequivalence Study of Two Formulations of Enalapril, at a Single Oral Dose of 20 mg (Tablets): A Randomized, Two-Way, Open-Label, Crossover Study in Healthy Volunteers. *Current Therapeutic Research*, 65, 1, 34-46.
- ^f Advanced Chemistry Development Inc. ACD/Labs 7.0, 7.09
- ^g logD was not available by ACD. Used ClogP instead.
- ^h S_T was not available by ACD. Used GSE instead.

Table 3.4
Physical Properties, Dose, and Human Intestinal Absorption Data for Saturated
Drugs

Drug Name	FA	D(mg)	Ref for FA and Dose	MP (°C)	Ref for MP	MW	logS _w	Ref for S _w	ClogP ^j
Acetazolamide	1.00	250	d	261	e	222	-2.36	e	-1.25
Acetylsalicylic acid	0.84	1200	a	135	e	180	-1.59	e	1.02
Allopurinol	0.90	300	b	350	e	136	-2.38	e	-0.86
Alprenolol	0.95	100	c	108	e	249	-2.98	h	2.65
Amphotericin B	0.03	3500	a	170	f, k	924	-3.09	e	-3.65
Azithromycin	0.37	500	a	114	e	749	-2.89	h	2.50
Aztreonam	0.01	500	a	227	f, k	435	-1.12	h	-0.40
Bromocriptine	0.28	1.5	a	218	g, k	654	-8.01	h	6.58
Bupropion	0.87	125	a	25	oil, f	240	-2.93	h	3.43
Camazepam	1.00	20	a	174	e	372	-4.63	h	3.64
Carbamazepine	1.00	1000	c	190	e	236	-4.12	c	1.98
Cefadroxil	1.00	500	a	197	f, k	363	-2.51	i	-2.31
Cefazolin	0.05	600	c	199	g, k	455	-3.33	c	-1.16
Cefoperazone	0.10	600	c	170	e	646	-4.00	c	-0.02
Cefoxitin	0.15	600	c	150	g	427	-3.61	c	-0.75
Chlorothiazide	0.49	150	a	350	e, k	296	-3.05	e	-0.31
Chlorpromazine	1.00	75	c	< 25	e	319	-5.10	e	5.8
Cisapride	1.00	13	a	109	g	466	-3.99	h	3.65
Clofibrate	0.97	1500	a	< 25	e	243	-3.62	h	4.12
Clomipramine	1.00	50	c	190	e	315	-6.03	c	5.92
Clozapine	1.00	450	c	183	g	309	-4.42	c	4.75
Cyclosporin	0.28	560	a	150	e	1202	-3.67	h	2.92
Cyproterone acetate	1.00	25	a	201	g	417	-4.80	h	3.54
Desipramine	1.00	50	a	25	g	266	-3.66	e	4.47
Diazepam	1.00	15	a	132	e	285	-3.76	e	3.16
Diclofenac	1.00	50	a	157	f	296	-5.10	e	4.32
Dicloxacillin	0.85	375	c	218	g, k	434	-4.23	h	2.8
Disulfiram	0.97	250	a	71.5	e	296	-4.86	e	3.88

Drug Name	FA	D(mg)	Ref for FA and Dose	MP (°C)	Ref for MP	MW	logS _w	Ref for S _w	ClogP ^j
Ethinylestradiol	1.00	30	a	183	e	296	-4.42	e	3.86
Felodipine	0.88	27.5	a	145	f	384	-6.28	h	5.58
Fenclofenac	1.00	400	a	112	e	297	-5.08	h	4.71
Flecainide	0.81	100	a	146	e	414	-5.35	h	4.64
Fluvastatin	1.00	6	a	195	g	411	-5.25	h	4.05
Fosinopril	0.36	10	a	151	i	564	-8.42	h	7.66
Furosemide	0.61	40	a	195	e	330	-3.65	e	1.87
Glyburide	1.00	3	a	169	e	358	-4.95	e	4.23
Griseofulvin	0.43	250	b	220	e	353	-4.61	e	1.75
Guanabenz	0.80	24	a	228	e, k	231	-4.49	h	2.96
Haloperidol	1.00	20	c	152	e	376	-4.43	e	3.85
Hydrocortisone	0.91	200	a	220	e	362	-3.05	e	1.70
Ibuprofen	0.95	400	a	76	e	206	-3.99	e	3.68
Imipramine	1.00	50	a	175	e	280	-4.19	e	5.04
Indomethacin	1.00	50	a	158	e	358	-5.58	e	4.18
Isoxicam	1.00	200	a	268	f, k	335	-3.52	h	1.59
Isradipine	0.92	13	a	169	f	371	-5.14	h	4.20
Ketoprofen	0.92	1013	a	94	e	254	-3.70	e	2.76
Labetalol	0.95	600	a	188	e	328	-3.45	e	2.50
Lamotrigine	0.98	127.5	a	217	f	256	-3.18	f	2.19
Lansoprazole	0.85	30	a	169	g, k	369	-5.58	i	3.07
Lovastatin	0.10	60	a	175	f	405	-6.01	f	4.30
Meloxicam	0.90	30	a	254	e, k	351	-4.07	h	2.28
Mexiletine	1.00	250	a	204	e	179	-3.86	h	2.57
Naproxen	0.99	250	a	153	e	230	-4.16	e	2.82
Nefazodone	1.00	100	a	84	e	470	-5.65	h	5.56
Nicardipine	1.00	25	c	137	e	480	-6.13	h	5.51
Nifedipine	1.00	45	c	173	e	346	-4.39	h	3.41
Nimodipine	1.00	30	c	125	g	419	-4.64	h	4.14
Nisoldipine	0.90	15	a	152	g	388	-5.63	h	4.86
Nitrendipine	0.88	20	a	158	g	360	-4.85	h	4.02
Nordazepam	0.99	10	a	216.5	e	270	-4.43	h	3.01
Olsalazine	0.24	2500	a	> 300	g	302	-6.75	h	4.50
Ondanstron	1.00	8	a	232	g	293	-4.29	h	2.72

Drug Name	FA	D(mg)	Ref for FA and Dose	MP (°C)	Ref for MP	MW	logS _w	Ref for S _w	ClogP ^j
Oxatomide	1.00	60	a	154	e	426	-6.43	h	5.64
Penicillin G	0.65	500	c	83	g	334	-1.83	h	1.75
Phenylbutazone	1.00	300	c	105	e	308	-3.81	e	3.38
Phenytoin	0.90	400	a	286	e	252	-3.90	e	2.08
Piroxicam	1.00	20	a	199	e	331	-4.16	e	1.89
Praziquantel	1.00	1960	a	136	e	312	-2.89	e	3.36
Probenecid	1.00	500	c	195	e	285	-4.57	h	3.37
Promazine	1.00	100	c	< 25	e	284	-4.30	e	4.9
Promethazine	1.00	112.5	c	60	e	284	-4.26	e	4.9
Propranolol	0.99	300	a	96	e	259	-3.62	e	2.75
Propylthiouracil	0.76	400	a	219	e	170	-2.15	e	-0.33
Quinidine	0.81	330	a	174	e	324	-3.36	e	2.79
Saccharin	0.88	2000	a	228	e, k	183	-1.66	e	0.72
Sotalol	0.95	16800	a	207	e	272	-1.10	h	-0.22
Spirolactone	0.73	125	a	135	e	417	-4.28	e	2.25
Sulfamethizole	0.85	750	c	208	e	270	-2.41	e	0.22
Sulfasalazine	0.59	2000	a	220	e, k	398	-5.28	h	3.83
Telmisartan	0.90	40	a	261	g	514	-9.32	h	7.46
Testosterone	1.00	20	a	155	e	288	-4.09	e	3.22
Tetracycline	0.65	750	c	173	e	444	-3.28	e	-0.91
Thiabendazole	0.90	500	d	300	e	201	-3.60	e	1.64
Thiacetazone	0.20	150	a	225	e, k	236	-3.43	e	0.88
Tolbutamide	1.00	1000	c	129	e	270	-3.39	e	2.5
Toremifene	1.00	120	a	109	g	406	-6.87	h	6.53
Trovafloxacin (CP99219)	0.88	200	a	246	f, k	416	-4.53	e	0.10
Valproicacid	1.00	600	a	25	g	144	-1.86	e	2.98
Venlafaxine	0.97	50	a	75	g	277	-3.27	h	3.27
Verapamil	1.00	120	a	< 25	e	455	-3.97	h	4.47
Viloxazine	0.98	200	a	178	g	237	-2.79	h	1.76
Warfarin	0.98	5	a	161	e	308	-4.26	e	2.89
Ximoprofen	0.98	30	a	178	e	261	-3.36	h	2.33
Xipamide	0.70	20	b	256	g	355	-3.79	e	1.89

- ^a Zhao *et al.*, 2001. Evaluation of human intestinal absorption data and subsequent derivation of a quantitative structure-activity relationship (QSAR) with the Abraham descriptors. *J. Pharm. Sci.*, 90, 749-784.
- ^b Sanghvi *et al.*, 2003. Predicting passive intestinal absorption using a single parameter. *QSAR Comb. Sci.*, 22, 247-257.
- ^c Willmann *et al.*, 2004. A physiological model for the estimation of the fraction dose absorbed in humans. *J. Med. Chem.*, 47, 4022-4031.
- ^d Hou *et al.*, 2007. ADME evaluation in drug discovery. 7. Prediction of oral absorption by correlation and classification. *J Chem Inf Model*, 47, 208-218.
- ^e Estimation Program Interface (EPI) Suites, EPA
- ^f *The Merck Index*, 13th ed.; Merck Research Laboratories, Whitehouse Station, 2001.
- ^g SciFinder Scholar, American Chemical Society
- ^h General Solubility Equation
- ⁱ Drugbank online. www.drugbank.ca
- ^j ClogP for Windows, v4.0 (Biobyte Corp.)
- ^k Decomposition temperature

3.10 Conclusion

Streamlining drug discovery programs and optimizing the oral bioavailability of lead candidates remain a significant challenge to the pharmaceutical industry. *In silico* models provide useful information on the physicochemical properties that determine passive transport through biological membranes. The control of these parameters can be used in designing and developing new compounds given their known relationship to good oral absorption. Absorption potential models (AP_{Balon} and MAP) that relate a compound's solubility, partition coefficient, and dose to drug absorption, provide a greater degree of insight into "drugability" during lead candidate selection. More recently, melting point has been correlated to intestinal absorption in the MPbAP model, where in general, low melting compounds will be better absorbed than high melting compounds. The MAP and MPbAP parameters can also be used to estimate at what maximum dose a compound will be well absorbed. The use of *in silico* models can facilitate the design and formulation of new drugs for maximum absorption efficiency.

CHAPTER 4: AN INTERESTING RELATIONSHIP BETWEEN DRUG ABSORPTION AND MELTING POINT

4.1 Introduction

The ability to predict the extent of passive intestinal drug absorption is very important for efficient lead candidate selection and development. Physicochemical-based absorption predictive models previously developed use solubility, partition coefficient and pKa as drug input parameters for intestinal absorption. Alternatively, this chapter looks at the relationship between melting point and passive transport for poorly soluble drugs. It is based entirely on the expression derived from the General Solubility Equation (GSE) that relates melting point to the *product* of intrinsic solubility and partition coefficient. Given that the melting point of a compound is one of the first and more reliable physical properties measured, it can be advantageously used as a guide in early drug discovery and development.

Rational drug design and automated *in vitro* screening have produced promising compounds with respect to intrinsic activity, yet their physicochemical properties are often not optimized to promote passive intestinal absorption. It is generally recognized that the pharmacokinetic profile of a drug is influenced by its physical chemical properties, *i.e.*, molecular weight, lipophilicity, polar surface area, hydrogen-bond donors

and acceptors, etc.¹⁻⁴ These molecular descriptors can be manipulated to obtain drugs with the desired physicochemical properties governing passive intestinal drug transport, *i.e.*, solubility and permeability.

A number of physicochemical and physiological factors affect oral drug absorption. Factors such as drug solubility, lipophilicity, dissolution, formulation, food composition, gastric emptying time, GI fluid volume, GI fluid pH, bile salts, intestinal motility, and specialized membrane transport can all affect absorption. Clearly, intestinal absorption is a complex process and any model that attempts to encompass all the physicochemical and physiological properties governing transport of drug molecules will not be straightforward. For poorly soluble drugs that are not subject to active or efflux transport mechanisms, a few simple physicochemical parameters are sufficient for determining the fraction of drug absorbed by passive transport.

Lipinski's "Rule of Five"⁵ and the Biopharmaceutics Classification System⁶ provide a qualitative and a semi-quantitative understanding, respectively, of how solubility and permeability affect oral absorption. Others have proposed predictive models that provide a more quantitative perspective of how aqueous solubility, S_w^{int} , partition coefficient, K_{ow} , and dose affect the extent of passive intestinal absorption.⁷⁻⁹ Another model utilizes the first-order absorption rate constant, intrinsic solubility, and particle size to determine the maximum absorbable dose.¹⁰ This chapter describes in detail the development of

another model using the melting point of a compound to predict the fraction of drug absorbed.

4.1.1 Absorption Potential

Dressman *et al.*⁷ and Balon *et al.*⁸ developed absorption potential, AP, models to estimate the intestinal absorption of drugs by passive transport. Dressman's absorption potential is calculated from S_w^{int} , K_{ow} , and the fraction of unionized drug at pH 6.5, F_{non} , luminal volume in liters, V , and administered dose in moles, D . The volume of the lumen is usually assumed to be 0.250 L.⁷ Balon's model is more quantitative and is based on the solubility of the drug in water at pH 6.8, $S_T^{6.8}$, and the distribution coefficient at the same pH, $K_D^{6.8}$, instead of their intrinsic counterparts.

$$AP_{Balon} = \log \left(\frac{S_T^{6.8} \cdot K_D^{6.8} \cdot V}{D} \right) \quad (1)$$

A sigmoidal relationship between the absorption potential and the human fraction of drug absorbed has been observed by Dressman for 7 drugs and Balon for 20 drugs.

4.1.2 Effect of pH on Transport for Saturated Solutions

The pH-dependence of the total solubility and the octanol-buffer distribution coefficient are well understood and can be reliably modeled on the basis of the intrinsic solubility,

intrinsic partition coefficient, pH and pKa values. Although it is not especially difficult to experimentally determine the pKa and log D values for compounds, it may not be practical to do so when thousands of compounds are being screened for passive intestinal absorption. A useful simplification that requires no prior knowledge of dissociation constants and pH has been put forward. In saturated solutions, Ni *et al.*¹¹ showed that as the total solubility, S_T , of a weak electrolyte increases with pH, there is an accompanying and proportionate decrease in the distribution coefficient, K_D , such that the product of the two ($S_T \cdot K_D$) is a constant and equal to the product of their intrinsic counterparts ($S_w \cdot K_{ow}$).

$$S_T \cdot K_D = S_w^{int} \cdot K_{ow} \quad (2)$$

This relationship assumes that ion pair partitioning and salt precipitation are negligible. The average absolute difference between the two products for the 25 acids, bases, and ampholytes that Ni *et al.* studied is 0.116 log units. This error is small relative to the typical errors associated with calculated solubility and partition coefficient values. The small error confirms the applicability of equation 2.

The basis for the relationship between the two products ($K_D \cdot S_T$ and $K_{ow} \cdot S_w^{int}$) is the concentration of the uncharged species in octanol. First, the distribution coefficient is the ratio of the total concentrations (*i.e.*, the sum of the concentrations of the unionized and ionized forms) of the drug in the octanol phase to that in the aqueous phase. That is:

$$K_D = \frac{[HA]_{oct} + [A^-]_{oct}}{[HA]_w + [A^-]_w} \quad (3)$$

where [HA] is the concentration of the unionized species and [A⁻] is the concentration of the ionized form, and the subscripts _{oct} and _w represent the octanol and aqueous phases, respectively. If it is assumed that the concentration of the ionized form in octanol is negligible, then the total concentration of the drug in octanol can be approximated by the concentration of the uncharged form. Therefore, the distribution coefficient can be simplified as:

$$K_D = \frac{[HA]_{oct}}{S_T} \quad (4)$$

or

$$S_T \cdot K_D = [HA]_{oct} \quad (5)$$

Secondly, since the intrinsic octanol-water partition coefficient only measures the unionized species in the two phases, the product of $S_w^{int} \cdot K_{ow}$ also results in a constant:

$$S_w^{int} \cdot K_{ow} = [HA]_w \left(\frac{[HA]_{oct}}{[HA]_w} \right) = [HA]_{oct} \quad (6)$$

Equations 5 and 6 show that the two products ($K_D \cdot S_T$ and $K_{ow} \cdot S_w^{int}$) approximate the concentration of the uncharged species in octanol. In saturated solutions this value is constant and independent of pH. Thus, it provides the basis for the equivalence of $K_D \cdot S_T$ and $K_{ow} \cdot S_w^{int}$ (*i.e.*, equation 2). The use of the terms S_w^{int} and K_{ow} provides an advantage since they are easier to measure and to calculate than S_T and K_D and consequently it is not necessary to consider the pKa of the drug. Furthermore, their use eliminates the potential inaccuracies of determining distribution coefficients and solubilities at a specific pH. It also avoids the inability of a single pH value to model the entire absorbing region of the small intestine where according to Willmann *et al.*¹² the pH can range from 5.0 to 7.5. This can translate into a 100-fold or more difference in solubility, depending on the pKa of the drug substance.

4.1.3 Modified Absorption Potential

Based on the above rationale, Sanghvi *et al.*⁹ proposed a modified absorption potential (MAP) that requires only S_w^{int} and K_{ow} as molecular input parameters. By combining equations 1 and 2 they get:

$$MAP = \log \left(\frac{S_w^{int} \cdot K_{ow}}{4 \cdot Dose} \right) \quad (7)$$

For the combined 27 compounds analyzed by Dressman and Balon, Sanghvi reported that the fraction of drug absorbed is correlated as well as or better with MAP than with AP. It should be emphasized that the above modified absorption potential is only valid for drugs that are in suspension in the GI fluid volume, as noted in a subsequent paper by Sanghvi *et al.*¹³ If the MAP is applied to drugs in solution, the intrinsic solubility term used in the MAP model would be an overestimate of the concentration of the uncharged species, resulting in an artificially high MAP value.

4.2 Methods

4.2.1 Compound Selection

Only passively transported drugs are evaluated in this study. Compounds known to have active or efflux transport mechanisms and compounds known to be extensively metabolized in the gut or liver are excluded from the data set. Low solubility drugs are defined here as those drugs that form saturated solutions in the gut. A drug is assumed to form a saturated solution if its molar solubility is less than the concentration of the dose in moles dispersed in 0.250 L of aqueous medium, *i.e.*, if

$$S_w^{\text{int}} < 4 \cdot \text{Dose} \quad (8)$$

Salts are excluded in this study since the General Solubility Equation (GSE)¹⁴ is only applicable to nonelectrolytes and the uncharged form of weak electrolytes.

4.2.1.1 Absorption Data

Experimentally derived human intestinal absorption data for 219 structurally diverse compounds were compiled from the literature.^{12, 13, 15} Due to the compound selection criteria for passively absorbed low solubility drugs, only 91 compounds are evaluated in the model and are listed in Table 4.1. If more than one fraction absorbed value is given, an average was used. Most of the doses were taken from these references. Additional sources are cited in the table. If multiple doses are available for a given compound, the average dose was taken. For doses given in mg/kg, a body weight of 70 kg was used. Some of the cephalosporin antibiotics are not available as oral drugs and thus their doses were not reported. Therefore, an average among typical oral doses ranging from 200 to 1000 mg¹⁶ is used for members of this class of compounds. Although the uptake of some cephalosporin antibiotics is mediated by PEPT1 transporters¹⁷ the seven cephalosporins in this data set were determined to be passively absorbed.^{12, 17}

4.2.1.2 Physical Data

Experimental melting point, MP, intrinsic aqueous solubility, S_w^{int} , and molecular weight, MW, values were obtained from the Estimation Programs Interface (EPI) Suite,¹⁸ SciFinder Scholar,¹⁹ the AQUASOL dATABASE²⁰, or the Merck Index,²¹ as well as from the literature sources mentioned in the previous section. The octanol-water partition coefficient was calculated using ClogP for Windows.²² Experimental solubility values were only available for 61 drugs, thus, solubility data for the remaining 32 drugs were estimated using the GSE. The melting temperatures for ceftazidime and cefmetazole were

estimated using EPI Suite since their experimental melting data could not be found. The experimental fraction absorbed data and the physical data of the 91 drugs analyzed in this study are listed in Table 4.1.

Table 4.1 Physical Properties, Dose and Human Intestinal Absorption Data

Drug Name	FA	Ref for FA	D(mg)	Ref for Dose	MP (°C)	Ref for MP	MW	logS _w	Ref for S _w	logP ^a
Acyclovir	0.22	b, c (avg)	350	b, c (avg)	255	g	225	-2.24	e	-2.52
Allopurinol	0.90	f	300	f	350	f	136	-2.38	g	-0.86
Alprenolol	0.95	b, c (avg)	100	b, c	108	g	249	-2.98	h	2.65
Bupropion	0.87	c	125	c (avg)	25	n	240	-3.23	c	3.43
Camazepam	1.00	c	20	c	174	g	372	-4.63	h	3.64
Carbamazepine	0.85	f, b (avg)	733	f, b (avg)	190	g	236	-4.12	b	1.98
cefamandole nafate	0.00	f	2000	f	190	j, d	462	-3.43	f	0.31
Cefazolin	0.05	b	600	i	199	j, d	455	-3.33	b	-1.16
Cefmetazole	0.10	b	600	i	330	g, r	472	-2.97	b	-1.28
Cefoperazone	0.10	b	600	i	170	g	646	-4.00	b	-0.02
Cefoxitin	0.15	b	600	i	150	j	427	-3.61	b	-0.75
Ceftazidime	0.02	b	600	i	350	g, r	546	-3.04	b	-6.22
Ceftizoxime	0.72	c	500	c	227	s	382	-2.47	h	0.95
chloramphenicol	0.90	f	1000	f	151	f	323	-2.11	f, g	1.28
chlorothiazide	0.19	f	250	f	342	d, f	296	-3.05	f, g	-0.31
Chlorpromazine	1.00	b	75	b (avg)	25	g	319	-5.10	b, g	5.8
Cisapride	1.00	c	12.5	c (avg)	109	j	466	-3.99	h	3.65
Clofibrate	0.97	c	1500	c	25	j	243	-3.40	e	4.12
Clomipramine	1.00	b	50	b	190	j	315	-6.03	b	5.92
Clozapine	1.00	b	450	b (avg)	183	j	309	-4.42	b	4.75

Drug Name	FA	Ref for FA	D(mg)	Ref for Dose	MP (°C)	Ref for MP	MW	logS _w	Ref for S _w	logP ^a
Desipramine	1.00	b, c, f	65	b, c	216	n, p	266	-3.66	f, g	4.47
Diazepam	0.985	b, c (avg)	15	b, c (avg)	132	g	285	-3.76	g	3.16
Diclofenac	1.00	b, c, f (avg)	50	b, c	157	n	295	-4.37	f	4.32
Dicloxacillin	0.85	b	375	b	218	j, d	470	-5.11	b	2.8
Diltiazem	0.92	b	180	b	214	j	415	-2.95	j	3.65
Disulfiram	0.97	c	250	c	71	g	296	-4.8596	c, g	3.88
Ethinylestradiol	1	c	30	c	183	g	296	-4.42	g	3.86
Etoposide	0.50	b, c	305	b, c (avg)	239	g	589	-3.47	e	-0.35
Felodipine	0.94	b, c	27.5	b, c	145	j	384	-5.68	c	5.58
Fenclofenac	1.00	c	400	c	112	g	297	-4.55	e	4.71
Flecainide	0.81	c	100	c	146	g	414	-5.35	h	4.64
Fluoxetine	0.80	f	30	f	158	f	309	-5.40	h	4.57
Fluvastatin	1.00	b, c	6	b, c (avg)	195	j	411	-5.25	h	4.05
Furosemide	0.65	b, c, f (avg)	40	b, c	295	g	331	-3.66	g	1.87
Glyburide	1.00	c	3	c (avg)	169	g	494	-5.09	g	4.23
Griseofulvin	0.43	f	250	f	220	f	353	-4.61	f	1.75
Guanabenz	0.78	b, c (avg)	24	b, c (avg)	228	d, g	231	-4.49	h	2.96
Haloperidol	1.00	b	20	b	152	g	376	-4.43	g	3.85
Hydrocortisone	0.90	b, c, f (avg)	175	b, c, f (avg)	220	g	362	-3.05	g	1.70
Ibuprofen	0.917	b, c, f (avg)	300	b, c, f (avg)	76	g	206	-3.99	g	3.68
Imipramine	0.98	b, c, f (avg)	50	b, c (avg)	175	g	280	-4.19	g	5.04
Indomethacin	0.99	b, c (avg)	50	b, c	158	g	358	-5.58	g	4.18
Isradipine	0.96	b, c (avg)	12.5	b, c (avg)	169	j	430	-5.14	h	4.20
Itraconazole	0.80	k	200	l	166	b	706	-5.85	l	6.50
Ketoprofen	0.96	b, c, f (avg)	112.5	b, c (avg)	94	g	254	-3.70	g	2.76

Drug Name	FA	Ref for FA	D(mg)	Ref for Dose	MP (°C)	Ref for MP	MW	logS _w	Ref for S _w	logP ^a
Labetalol	0.95	b, c, f	600	b, c	188	g	328	-3.45	g	2.50
Lansoprazole	0.85	c	30	c	169	j, d	369	-5.18	h	4.24
Meloxicam	0.90	c	30	c	255	d, g	351	-4.08	h	2.28
Methadone	0.80	c	6.71	m (avg)	100	j	309	-4.42	h	4.17
Methylprednisolone	0.82	b, c	42	b, c	233	g	374	-3.49	g	1.70
Naproxen	0.99	b, c, f	250	b, c	153	g	230	-4.16	g	2.82
Nefazodone	1.00	c	100	c	84	g	470	-5.65	h	5.56
Nicardipine	1.00	b	25	b (avg)	137	g	466	-5.33	e	5.51
Nifedipine	1.00	b	45	b (avg)	173	g	346	-3.79	b	3.41
Nimodipine	1.00	b	30	b	125	j	418	-4.24	b	4.14
Nisoldipine	0.95	b, c (avg)	15	b, c (avg)	152	j	388	-5.63	h	4.86
Nitrendipine	0.94	b, c (avg)	20	b, c	158	j	360	-4.85	h	4.02
Nordazepam	0.99	b, c	10	b, c	217	g	270	-4.43	h	3.01
Norfloxacin	0.47	b, c, f, m (avg)	400	b, c, f, m	221	n	319	-3.06	n	-0.99
Olanzapine	0.75	f	10	f	195	j	312	-5.09	h	3.89
Olsalazine	0.17	c, f (avg)	2500	c, f (avg)	> 300	j	302	-7.42	e	4.50
Ondansetron	1.00	b, c, f	8	b, c, f	232	j	293	-4.29	h	2.72
Oxatomide	1.00	c	60	c	154	g	426	-6.43	h	5.64
Oxazepam	0.97	f	15	f	206	g	287	-3.97	f	2.29
Pentazocine	1.00	b	50	b	146	g	285	-5.38	h	4.67
Phenylbutazone	1.00	b	300	b	105	g	308	-3.81	b, g	3.38
Phenytoin	0.90	b, c, f	250	b, c, f (avg)	286	g	252	-3.90	g	2.08
Pindolol	0.87	c	1050	c	171	g	248	-2.45	h	1.49
Piroxicam	0.99	f	20	f	199	g	331	-4.16	g	1.89
Praziquantel	1.00	c	1960	c	136	g	312	-2.89	g	3.36
Probenecid	1.00	b	500	b	195	g	285	-4.02	b	3.37
Promazine	1.00	b	100	b	25	g, q	284	-4.30	b	4.90
Promethazine	1.00	b	113	b	60	g	284	-4.26	b, g	4.90

Drug Name	FA	Ref for FA	D(mg)	Ref for Dose	MP (°C)	Ref for MP	MW	logS _w	Ref for S _w	logP ^a
				(avg)						
Propranolol	0.945	b, c (avg)	300	b, c	96	j	259	-2.96	h	2.75
Quinidine	0.805	b, c, f (avg)	330	b, c, f	174	g	324	-3.42	c, g (avg)	2.79
Spironolactone	0.73	c	125	c (avg)	135	g	417	-4.28	g	2.25
Sulfamethizole	0.85	b	750	b (avg)	208	j	270	-2.41	b	0.22
Sulindac	0.9	c	200	c	183	g	356	-4.24	h	3.16
Telmisartan	0.9	c	40	c	262	n	514	-9.33	h	7.46
Tenidap	0.895	c, f (avg)	116	c, f (avg)	230	j, d	321	-3.49	h	1.94
Testosterone	0.99	b, c, f (avg)	20	b, c, f	155	g	288	-4.09	g	3.22
Tetracycline	0.65	b	750	b (avg)	173	g	444	-3.28	b	-0.91
Thiacetazone	0.2	c	150	c	225	g	236	-3.43	g	0.88
Tolbutamide	0.93	b, c (avg)	1000	b	129	g	270	-3.27	b	2.50
Toremifene	1.00	c	120	c	109	j	406	-6.87	h	6.53
Trapidil	0.96	c	275	o	100	g	205	-2.46	h	2.21
Trimethoprim	0.97	f	160	f	201	g	290	-2.86	f	0.88
Valproic Acid	1.00	b, c	600	b, c	25	n, q	144	-2.48	h	2.98
Venlafaxine	0.97	c	50	c	103	j	277	-3.55	h	3.27
Viloxazine	0.98	c	200	c	178	j	237	-2.79	h	1.76
Ximoprofen	0.98	c	30	c	178	g	261	-3.36	h	2.33
Xipamide	0.70	f	20	f	256	j	355	-3.79	g	1.89

^a ClogP for Windows, v4.0 (Biobyte Corp.)

^b Willmann *et al.*, 2004. A physiological model for the estimation of the fraction dose absorbed in humans. *J. Med. Chem.*, 47, 4022-4031.

^c Zhao *et al.*, 2001. Evaluation of human intestinal absorption data and subsequent derivation of a quantitative structure-activity relationship (QSAR) with the Abraham descriptors. *J. Pharm. Sci.*, 90, 749-784.

^d decomposition temperature

^e AQUASOL dATABASE of aqueous solubility

^f Sanghvi *et al.*, 2003. Predicting passive intestinal absorption using a single parameter. *QSAR Comb. Sci.*, 22, 247-257.

^g Estimation Program Interface (EPI) Suites, EPA

^h General Solubility Equation

ⁱ cephalosporins not available as oral dose so typical oral dose is used

^j SciFinder Scholar, American Chemical Society

^k Hou *et al.*, 2007. ADME evaluation in drug discovery. 7. Prediction of oral absorption by correlation and classification. *J Chem Inf Model*, 47, 208-218.

^l Branchu *et al.*, 2007. A decision-support tool for the formulation of orally active, poorly soluble compounds. *Eur. J. Pharm. Sci.*, 32, 128-139.

^m Physicians' Desk Reference, 56th ed.; Medical Economics Company, Inc., Montvale, 2002.

ⁿ *The Merck Index*, 13th ed.; Merck Research Laboratories, Whitehouse Station, 2001.

^o Dose taken from online patent www.patentstorm.us/patents/6015578-description.html

^p Compound is liquid at room temperature. A MP of 25°C is given to liquid solutes in order to eliminate the crystalline solubility term in the GSE

^q Estimated melting temperature from EPI Suites

^r Yalkowsky *et al.*, 2006. A 'Rule of Unity' for human intestinal absorption. *Pharm. Res.*, 23, 2475-2481.

4.3 Results & Discussion

4.3.1 Modified Absorption Potential for Saturated Compounds (MAP)

Sanghvi's modified absorption potential assumes the drug is completely dissolved or reaches its solubility in the gut. This represents the best case scenario. Obviously, if this condition is not met, absorption will be altered. The application of the MAP at saturation to 91 passively absorbed low solubility compounds is illustrated in Figure 4.1. The figure can be divided into four quadrants by a horizontal line at 50% absorption and a solid vertical line at $\text{MAP} = 0$, that is, $\log(S_w^{\text{int}} \cdot K_{ow}) = \log(4D)$. Compounds with MAP values greater than zero ($\log(S_w^{\text{int}} \cdot K_{ow}) > \log(4D)$) are expected to be well absorbed while those that have MAP values less than zero ($\log(S_w^{\text{int}} \cdot K_{ow}) < \log(4D)$) should be poorly absorbed. In fact, about 92% of the drugs fall into the upper right and lower left quadrants.

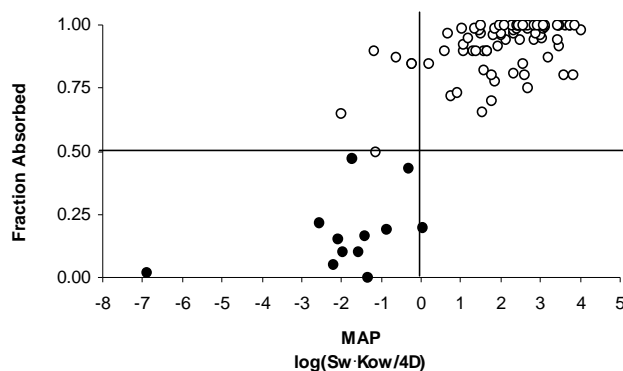


Figure 4.1: Relationship between MAP and Fraction Absorbed. (●) Compounds with $FA < 0.5$. (○) Compounds with $FA > 0.5$.

The six compounds in the upper left quadrant (allopurinol, carbamazapine, etoposide, pindolol, sulfamethizole, and tetracycline) and the one drug in the lower right quadrant (thiacetazone) cannot be explained based on any apparent pattern among their structural features. Active and efflux transport mechanism, again, are not expected for these compounds. In examining the effects of using calculated logP versus experimental logP values in the model, there was no difference in the correlation between MAP and FA. All seven of the outliers had experimental solubility data.

Errors may come from any one or a combination of sources from: solubility, partition coefficient, dose, human absorption data, or simply from the failure of the model. In addition, it is not possible to know what, if any, the effects of formulation factors are on the experimental absorption data. Formulations that lead to supersaturated solutions in the

gut may increase the amount absorbed. A prediction rate of 92% is very good in light of the different degrees of uncertainty for all of the measured data.

The effectiveness of a delineator of $MAP = 0$ in Figure 4.1, indicates that for at least 50% absorption,

$$MAP = \log\left(\frac{S_w^{int} \cdot K_{ow}}{4 \cdot Dose}\right) \geq 0 \quad (9)$$

or

$$\log(S_w^{int} \cdot K_{ow}) \geq \log(4 \cdot Dose) \quad (10)$$

Equation 10 gives rise to the product of S_w^{int} and K_{ow} vs. $4 \cdot Dose$ for the same 91 drugs plotted in Figure 4.2. As in Figure 4.1, the filled and open circles represent compounds with $FA < 0.5$ and $FA \geq 0.5$, respectively. The solid line with a slope of unity is described by equation 10 when $\log(S_w^{int} \cdot K_{ow}) = \log(4 \cdot Dose)$. This corresponds to the vertical line in Figure 4.1 at $MAP = 0$. Clearly the vast majority of the well absorbed compounds lie to the right of the diagonal line.

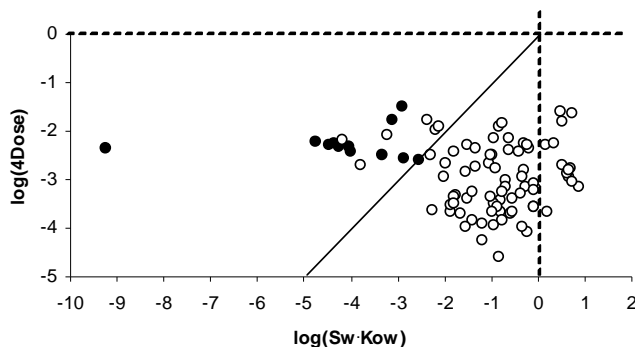


Figure 4.2. Relationship between $S_w^{int} \cdot K_{ow}$, Dose and Fraction Absorbed. The line is described by Equation 10 with a slope of 1 and intercept of 0. (●) Compounds with $FA < 0.5$. (○) Compounds with $FA \geq 0.5$.

Figure 4.2 provides a quantitative perspective of the roles of the *product* of solubility and partition coefficient and dose on fraction absorbed. Without sufficient drug available in solution, absorption will be limited. Inadequate membrane partitioning of the solute will also reduce the extent of passive intestinal absorption. A dose that is significantly oversaturated (*i.e.*, doses above the diagonal line) will likely lead to a decrease in absorption efficiency. According to Curatolo,²³ the hallmarks of a well absorbed drug are high solubility and moderate lipophilicity. While there is no question that drugs with these physicochemical characteristics typically do not have problems with absorption, Figure 4.2 indicates that for discrete combinations of solubility and partition coefficient values, (*i.e.*, the product of S_w^{int} and K_{ow}) even drugs that are poorly soluble or very lipophilic have the potential of being well absorbed if given at a sufficiently low dose.

The significance of dose in the MAP model might be better appreciated under the following context. For a given compound, if the logarithm of the product of S_w^{int} and K_{ow} is greater than the logarithm of $4 \cdot \text{Dose}$, the drug is likely to be well absorbed. Or put another way, the absorption potential of a drug with the requisite solubility and partitioning properties (*i.e.*, $\log(S_w^{int} \cdot K_{ow}) \geq \log(4 \cdot \text{Dose})$) is not expected to be limited by a high dose. In this regard, the dose quantifies what is meant by adequate values of aqueous solubility and membrane partitioning for improved drug absorption. Interestingly, MAP is analogous to the concept of the maximum absorbable dose, MAD, developed by Johnson and Swindell¹⁰ However, while MAD requires biological data, MAP only requires physicochemical data.

4.3.2 General Solubility Equation

Jain and Yalkowsky¹⁴ revised the General Solubility Equation (GSE) in which the aqueous solubility of an unionized organic compound is related to its octanol-water partition coefficient and its melting point by,

$$\log S_w^{int} = 0.5 - 0.01(MP - 25) - \log K_{ow} \quad (11)$$

where MP is the melting point of the drug in degrees Celsius. Rearranging this equation gives

$$\log(S_w^{int} \cdot K_{ow}) = 0.5 - 0.01(MP - 25) \quad (12)$$

This enables us to replace the S_w^{int} and K_{ow} product in Equation 7 with the MP term.

Although solubility and dissolution rates have typically been correlated with melting

temperatures, the melting point of a drug has not been used as a predictive tool for oral absorption efficiency of poorly soluble drugs. Given that the melting point of a compound is one of the first and more reliable physical properties measured, it can be advantageously used to guide the screening and selection of lead compounds.

4.3.3 Melting Point-Based Absorption Potential (MPbAP)

Dressman's ⁷, Balon's ⁸ and Sanghvi's ⁹ passive intestinal drug absorption models are based on a few physical parameters. Here, we distill the model down to one fundamental physical property and introduce a simpler yet meaningful tool to evaluate oral absorption efficiency. Replacing the log of the product of S_w^{int} and K_{ow} in Equation 7 with the right-hand side of Equation 12 results in the melting point-based absorption potential, MPbAP:

$$MPbAP = 0.5 - 0.01(MP - 25) - \log(4 \cdot Dose) \quad (13)$$

where the dose is in moles. Note that the above equation is applicable only if the dose exceeds the amount of drug that can be dissolved in 250 ml of water. Equation 13 and Figure 4.3 describe this interesting relationship between the fraction of drug absorbed, the dose, and melting point.

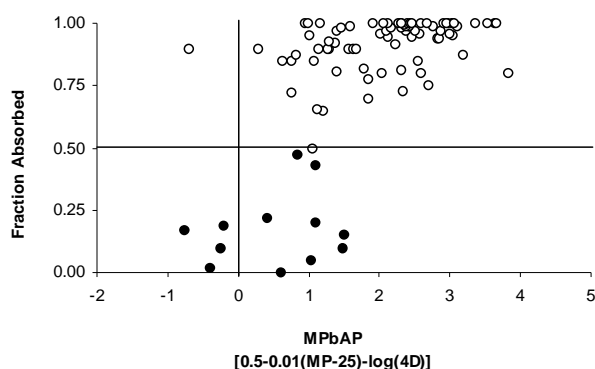


Figure 4.3. Relationship between MPbAP and Fraction Absorbed. (●) Compounds with FA < 0.5. (○) Compounds with FA > 0.5.

Figure 4.3 is analogous to Figure 4.1, where a vertical line at MPbAP = 0 and a horizontal line at FA = 0.5 create four quadrants with a delineator that discriminates between well-absorbed and poorly-absorbed drugs. Again most compounds with MPbAP values greater than 0 are shown to be well absorbed ($FA \geq 0.50$) and fall in the upper right quadrant while those that are poorly absorbed tend to fall in the lower left quadrant and have MPbAP values less than 0. Using a delineator at MPbAP = 0 gives 90% correct designations of drugs falling in the upper right and lower left quadrants.

The prediction rate of the MPbAP model can be considered quite good given the additional assumptions of the GSE. Two of the outliers (allopurinol and thiacetazone) in Figure 4.3 are the same as in Figure 4.1 while the other seven outliers may be attributed to the lack of exactness of the GSE, particularly for the four cephalosporin compounds having the only common structural features observed among the outliers (acyclovir,

allopurinol, cefamandole nafate, cefoperazone, ceftioxin, cefazolin, griseofulvin, norfloxacin, and thiacetazone).

It is also important to note that the General Solubility Equation assumes the melting point of the crystal does not change in the presence of water. In addition, if a drug has a true melting point that is significantly higher than the decomposition temperature, the GSE may overestimate the solubility and shift the drug to higher MPbAP values. None of the melting temperatures for the outliers were reported as decomposition temperatures. Salts were excluded in the study since the GSE is only applicable to nonelectrolytes and the uncharged form of weak electrolytes.

4.3.4 Melting Point, Dose and Fraction Absorbed

The relationship illustrated in Figure 4.3 may be interpreted in a somewhat more intuitive manner if we evaluate the combined effects of melting temperature and dose on the fraction absorbed. In order to observe their individual roles in MPbAP, they are plotted separately in Figure 4.4 where filled circles represent compounds with $FA < 0.5$ and open circles are compounds with $FA \geq 0.5$. From Figure 4.3 we've distinguished between efficient and poor absorption using $MPbAP = 0$. When $MPbAP \geq 0$, equation 13 becomes

$$[0.5 - 0.01 \cdot (MP - 25)] - \log(4 \cdot Dose) \geq 0 \quad (14)$$

which is analogous to Equation 9. Rearranging gives

$$0.75 - 0.01MP \geq \log(4 \cdot Dose) \quad (15)$$

which describes the condition for a minimum of 50% absorption. Equation 15 is plotted as the line with a slope of -0.01 and a y-intercept of 0.75 in Figure 4.4.

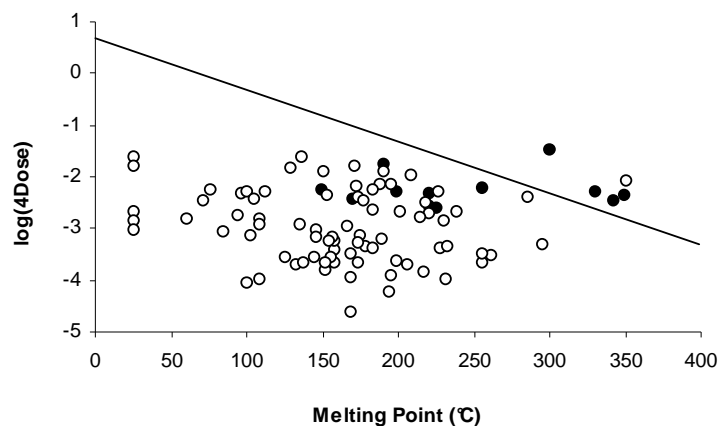


Figure 4.4. Relationship between Melting Point, Dose and Fraction Absorbed. The line is described by Equation 15 with a slope of -0.01 and intercept 0.75. (●) Compounds with FA < 0.50. (○) Compounds with FA ≥ 0.50. Some data points are covered.

It is clear that most of the well absorbed drugs fall below the line. Figure 4.4 is analogous to Figure 4.2 and can be interpreted in the same way but using one term, MP, instead of two terms, S_w^{int} and K_{ow} . Based on the GSE, the lower the melting temperature, the greater is the product of S_w^{int} and K_{ow} . Therefore, for any given dose, lower melting compounds are more likely to be well absorbed than higher melting compounds, just as

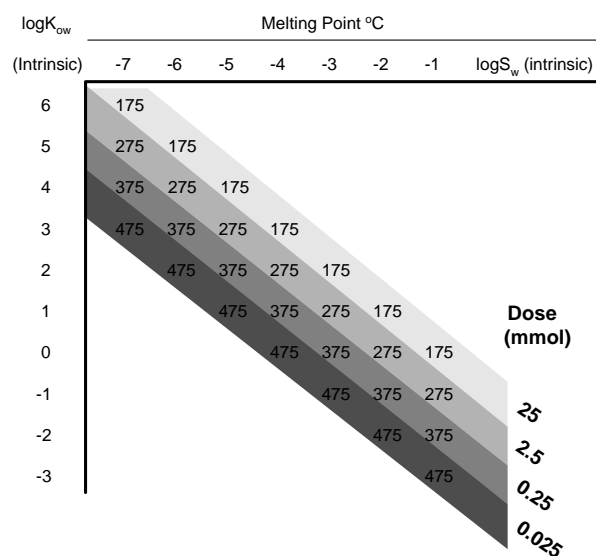
compounds that have greater $S_w^{int} \cdot K_{ow}$ values are more likely to be well absorbed than compounds with lower $S_w^{int} \cdot K_{ow}$ products. For a minimum of 50% absorption, the MP term of Equation 15 or the product of S_w^{int} and K_{ow} of Equation 10 must be greater than $4 \cdot \text{Dose}$. For example, using the diagonal line in Figure 4.4 as the cutoff, a drug with a melting point of 275 °C would be expected to have good absorption up to a dose of 2.5 mmoles, versus a similar drug with a melting point of 375 °C that can only be dosed up to 0.25 mmoles for adequate absorption. For a given dose level, every one hundred degrees increase in melting temperature brings the drug ten times closer to intersecting the point of decreased absorption efficiency (*i.e.*, the cut-off line).

Again, the significance of dose can be better understood in the following perspective. The fraction absorbed is independent of dose for drugs that are completely dissolved in the GI lumen. At high enough doses the GI lumen becomes saturated. Beyond this point, increasing the dose reduces absorption efficiency. The MPbAP model, as well as the MAP model, defines the maximum dose to achieve a minimum of 50% absorption.

The MPbAP model essentially collapses the two key physicochemical properties of passive intestinal absorption into a single, more easily measured property. While the convenience of the model allows the use of melting point to estimate fraction absorbed, fundamentally, the prediction is still based on the product of solubility and partition coefficient. Table 4.2 illustrates the interdependencies of S_w^{int} , K_{ow} , MP, and Dose in determining FA. If the solubility and partition coefficient values, found along the

horizontal and vertical axes, respectively, are known, then the corresponding melting temperature can be found in the table. Likewise, if the melting point of a drug is known, the product of S_w^{int} and K_{ow} is defined. The various combinations of solubility and partition coefficients can be determined.

Table 4.2
Interrelationship of Solubility, Partition Coefficient, Melting Point, and Dose for at Least 50% Absorption



The dose requirement for a minimum of 50% absorption as described by Equations 10 and 15 should be less than the product of S_w^{int} and K_{ow} or the MP term, respectively.

Combining Table 4.2 with dose levels completes the prediction of fraction absorbed. For

a 275 °C melting drug, the maximum acceptable dose for 50% absorption is 2.5 mmoles. Higher doses for a 275 °C melting drug will lead to decreased absorption efficiency and lower doses should lead to improved absorption efficiency. Another way to look at it is drugs with a dose of 2.5 mmoles will not be well absorbed if they have melting temperatures greater than 275 °C or have a value for the product of the logarithm of S_w^{int} and K_{ow} that is less than -2. Drugs that have melting temperatures of 175 °C should be well absorbed up to a maximum dose of 25 mmoles. Basically, the lower the melting point, the less likely that absorption will be limited by dose. Translating melting temperatures or dose values into solubility and partition coefficient values is easily accomplished by referring to Table 4.2.

4.4 Conclusion

Sanghvi's modified absorption potential has expanded our appreciation of the balancing act that solubility, partitioning, and dose play on passive absorption. In general, if the product of S_w^{int} and K_{ow} is greater than 4 times the dose, the compound is expected to be at least 50% absorbed. The ability to predict the extent of absorption is further facilitated by the General Solubility Equation which combines the product of aqueous solubility and membrane partitioning into one term. In spite of the complex process of intestinal absorption, the MPbAP model describes an interesting and potentially useful relationship between the fraction absorbed and a drug's melting point. In this model, the melting point acts as a surrogate for the product of solubility and partition coefficient and it allows one

to assess whether a drug is likely to be well absorbed or not at a given dose level. In general, low melting compounds will be better absorbed than high melting compounds. For every one hundred degrees increase in melting temperature, there is a ten-fold decrease in the maximum dose that will provide at least 50% absorption. Again, the interdependencies of melting point, solubility, partition coefficient, and dose in determining fraction absorbed are illustrated in Table 4.2. The MPbAP model may be a convenient tool to help facilitate rational drug design and development and provide a means to rank-order lead candidates in a more systematic and meaningful context. Appreciation for the dose limit to achieve at least 50% absorption has many implications on development time and costs.

CHAPTER 5: PREDICTING AQUEOUS SOLUBILITY: The Role of Crystallinity

5.1 Introduction

Various methods of predicting the aqueous solubility of a drug or drug-like substance have been reported. Most estimation approaches employ multiple linear regression models that are based on group contributions and require knowledge of the chemical structure of the solute. Molecular simulation algorithms can also be used to predict solubility but they are relatively slow as they involve a considerable computational load. Other methods, such as artificial neural networks, which are strictly computational approaches and do not involve any physical models, have been proposed. Although many of these models provide reasonably accurate predictions, they are limited in that they require the fitting of parameters to specific test sets and thus lack general applicability. From a philosophical point of view, the use of fewer terms that are intuitively obvious or that are thermodynamically sound is preferred.

The General Solubility Equation (GSE)¹ is a simple equation that does not require regression-generated coefficients and only involves two physicochemical properties. Jain *et al.*² have shown that the GSE, which is semi-empirically derived from thermodynamic

principles, provides reasonably accurate solubility predictions (AAE 0.576) for 1642 compounds. It is widely used in the pharmaceutical industry to predict solubility.

Box and Comer³ studied 86 drugs and compared their experimentally measured solubility values to solubility predictions based on measured octanol-water partition coefficients alone. They show that, in general, solubility predictions using $\log K_{ow}$ for lower and higher melting compounds tend to be under- and over-predicted, respectively. This paper compares the solubility predictions of the same data set using the General Solubility Equation to those values predicted by Box and Comer. By accounting for the crystal lattice energy and the aqueous activity coefficient of the drug, the GSE should make more accurate solubility predictions.

5.2 Method

Experimental intrinsic aqueous solubility, S_w^{int} , partition coefficient, K_{ow} , and melting point, MP, data for 86 drugs were compiled by Box and Comer³. For those compounds that did not have a melting point, or if the reported melting point was not of the free acid or free base, melting points were obtained from the literature sources referenced in Table 5.1. Calculated $\log K_{ow}$ values, using ClogP for Windows⁴, are also included in the table.

The predicted intrinsic aqueous solubility value for each compound is calculated using the General Solubility Equation and is expressed as:

$$\log S_w^{\text{int}} = 0.5 - 0.01(MP - 25) - \log K_{ow} \quad (1)$$

The average absolute error for calculations by Box and Comer³ and the GSE are compared.

5.3 Results & Discussion

Log K_{ow} and/or group contribution approaches have been the most common methods of estimating solubility in the past. In general, there is an inverse relationship between solubility and partition coefficient, especially for liquid solutes. Hansch *et al.*⁵ showed that for a large number of organic liquids, the aqueous solubility can be accurately predicted based on log K_{ow} alone, by

$$\log S = A \log K_{ow} + B \quad (2)$$

where A and B are constants that depend on the data set considered.

In a similar fashion, Box and Comer³ fitted their data to Equation 2 and obtained a relationship between solubility and measured octanol-water partition coefficient given by,

$$\log S_0 = -1.03 \log P - 0.54 \quad (3)$$

They conclude that higher melting drugs, or compounds having a greater number of hydrogen bond donors and acceptors, tend to be less soluble than predicted by their equation, and lower melting drugs, or compounds having a lower number of H-bond donors and acceptors, tend to be more soluble than predicted. Box and Comer's observations of the under- and over-predicted solubility values based on $\log K_{ow}$ alone, is evidence of the need to include some measure of crystallinity for solid solutes.

Researchers have studied the relationships of solubility to molecular weight, number of hydrogen bond donors and acceptors, polar surface area, and melting point, *etc.* The significance and advantage of including the melting point in the model is that it accounts for the lattice interaction energies of crystalline drugs. It is derived from the Clausius-Clapeyron equation and it does not co-vary with $\log K_{ow}$ to the extent that many other parameters like molecular weight and polar surface area do. For example, isomers such as anthracene and phenanthracene which have identical $\log K_{ow}$ values, often have significantly different melting points.

The aqueous solubility of a crystalline solute is governed by three major thermodynamic factors: (a) the difference between the adhesive and cohesive interactions of water and solute, which determines the aqueous activity coefficient (b) the intermolecular interactions associated with the crystal lattice, and (c) the entropy of mixing. The GSE combines the roles of crystallinity (as reflected by the melting point term), aqueous

activity coefficient (as reflected by the octanol-water partition coefficient), and entropy of mixing (as reflected by a constant that describes the comparable solubilities of liquid solutes in octanol) to estimate the aqueous solubility of organic nonelectrolytes.

Table 5.1 lists the compounds under study along with their physicochemical data, in the order they were presented in the Box and Comer paper³. The predicted solubilities and associated errors for both calculations are reported in Table 1 for 81 of the compounds considered. (As is noted in the footnote, several of the drugs were eliminated because no melting point was reported for the uncharged species). It can be seen from Table 5.1 that over 70 percent of the solubilities are more accurately predicted by the GSE than by the Box and Comer calculation. The average absolute error (AAE) for Box and Comer's solubility predictions for these compounds is 1.20 log units as compared to the GSE's AAE of 0.78. There was no difference observed in the error if the GSE used calculated or experimentally measured log P values.

Note that the GSE is only applicable to nonelectrolytes or the uncharged form of weak electrolytes. In other words, the GSE provides a researcher with an estimate of the equilibrium solubility of the free acid or free base. It is not applicable to ionized salts or zwitterions. One of the main assumptions of the GSE is that the crystal properties of the solute, and thus its melting point, are not affected by the presence of water. This also means that the true melting point must not be confused with melting temperatures of salts, hydrates, or polymorphs, as well as decomposition temperatures.

Table 5.1 Properties and Solubility Predictions of Compounds Studied by Box and Comer

Compound	MP (°C)	ClogP^e	Observed logP	Observed logS₀	logS_{GSE}	Absolute Error	logS_{Box&Comer}	Absolute Error
1-naphthol	95	2.65	2.85	-1.98	-2.85	0.87	-3.48	1.50
2-naphthoic acid	186	3.06	3.28	-3.78	-4.17	0.39	-3.92	0.14
4-hydroxybenzoic acid	215	1.56	1.58	-1.45	-2.96	1.51	-2.17	0.72
alprenolol	58 ^{1, a}	2.65	3.10	-2.63	-2.48	0.15	-3.73	1.10
amantadine	180 ^{2, b}	2.00	2.41	-1.86	-3.05	1.19	-3.02	1.16
amiodarone	n/a ²	8.93	7.57	-8.17				
amitriptyline	< 25	4.85	5.04	-4.39	-4.35	0.04	-5.73	1.34
amodiaquin	208 ³	4.51	4.20	-5.94	-5.84	0.10	-4.87	1.07
astemizole	149	6.09	5.70	-5.93	-6.83	0.90	-6.41	0.48
atenolol	147	-0.11	0.22	-1.29	-0.61	0.68	-0.77	0.52
benzocaine	92	1.92	1.89	-2.23	-2.09	0.14	-2.49	0.26
benzoic acid	122	1.88	1.87	-1.61	-2.35	0.74	-2.47	0.86
carprofen	198	3.98	4.29	-4.71	-5.21	0.50	-4.96	0.25
chlorpheniramine	< 25	3.15	3.39	-2.66	-2.65	0.01	-4.03	1.37
chlorpromazine	25	5.80	5.40	-5.08	-5.30	0.22	-6.10	1.02
chlorprothixene	98	5.48	5.48	-6.30	-5.71	0.60	-6.18	0.12
chlorzoxazone	192	1.87	2.11	-2.61	-3.04	0.43	-2.71	0.10
deprenyl (selegiline)	< 25	2.52	2.90	-2.52	-2.02	0.50	-3.53	1.01
desipramine	< 25	4.47	4.21	-3.44	-3.97	0.53	-4.88	1.44
diclofenac	284	4.32	4.51	-5.45	-6.41	0.96	-5.19	0.26

Compound	MP (°C)	ClogP ^e	Observed logP	Observed logS ₀	logS _{GSE}	Absolute Error	logS _{Box&Comer}	Absolute Error
diltiazem	n/a ²	3.65	2.89	-2.94				
diphenhydramine	< 25	3.54	3.44	-2.93	-3.04	0.11	-4.08	1.15
flufenamic acid	134	4.88	5.56	-5.35	-5.47	0.12	-6.27	0.92
fluoxetine	< 25	4.57	4.61	-3.92	-4.07	0.15	-5.29	1.37
flupenthixol	n/a ²	4.35	4.68	-4.02				
flurbiprofen	111	3.75	4.16	-4.11	-4.11	0.00	-4.82	0.71
furosemide	295	1.87	2.56	-4.23	-4.07	0.16	-3.18	1.05
haloperidol	152	3.85	4.30	-5.47	-4.62	0.85	-4.97	0.50
ibuprofen	76	3.68	3.97	-3.61	-3.69	0.08	-4.63	1.02
imipramine	< 25 ^{2,c}	5.04	4.42	-4.21	-4.54	0.33	-5.09	0.88
lidocaine	69	1.95	2.44	-1.85	-1.89	0.03	-3.05	1.20
maprotiline	93	4.52	4.85	-4.69	-4.70	0.01	-5.54	0.85
meclizine	n/a ²	6.73	6.20	-6.49				
meclofenamic acid	257	5.92	5.90	-6.86	-7.74	0.88	-6.62	0.24
mefenamic acid	231	4.94	5.33	-6.34	-6.50	0.16	-6.03	0.31
metoclopramide	147	2.21	2.74	-3.59	-2.93	0.66	-3.36	0.23
metoprolol	120	1.35	1.95	-1.21	-1.80	0.59	-2.55	1.34
miconazole	161 ⁴	5.81	5.34	-5.62				
nadolol	130	0.38	0.71	-1.57	-0.93	0.64	-1.27	0.30
naproxen	153	2.82	3.24	-4.14	-3.60	0.54	-3.88	0.26
niflumic acid	203	3.79	3.88	-4.47	-5.07	0.60	-4.54	0.07
nortriptyline	58 ^{2,a}	4.31	4.39	-3.99	-4.14	0.15	-5.06	1.07

Compound	MP (°C)	ClogP^e	Observed logP	Observed logS₀	logS_{GSE}	Absolute Error	logS_{Box&Comer}	Absolute Error
orphenadrine	< 25	3.99	3.84	-3.17	-3.49	0.32	-4.50	1.33
papaverine	148	3.77	2.95	-4.30	-4.50	0.20	-3.58	0.72
paracetamol (acetaminophen)	170	0.49	0.46	-1.00	-1.44	0.44	-1.01	0.01
phenobarbital	174	1.37	1.47	-2.28	-2.36	0.08	-2.05	0.23
phenylbutazone	105	3.38	3.25	-4.39	-3.68	0.71	-3.89	0.50
phthalic acid	230 ³	0.73	0.85	-1.49	-2.28	0.79	-1.42	0.07
pindolol	169	1.49	1.83	-3.79	-2.43	1.36	-2.42	1.37
pramoxine	< 25	4.17	3.56	-3.02	-3.67	0.65	-4.21	1.19
probenecid	195	3.37	3.70	-4.86	-4.57	0.29	-4.35	0.51
procaine	61	2.54	2.14	-1.72	-2.40	0.68	-2.74	1.02
prochlorperazine	< 25	4.90	4.88	-4.87	-4.40	0.47	-5.57	0.70
promethazine	60	4.90	4.56	-4.19	-4.75	0.56	-5.24	1.05
propranolol	96	2.75	3.48	-3.50	-2.96	0.54	-4.12	0.62
pyrimethamine	234	2.91	2.69	-4.10	-4.50	0.40	-3.31	0.79
quinine	57	2.79	3.50	-2.81	-2.61	0.20	-4.15	1.34
sertraline	< 25	5.35	4.30	-4.84	-4.85	0.01	-4.97	0.13
sulindac	183	3.16	3.42	-4.52	-4.24	0.28	-4.06	0.46
thyroxine (a)	236 ³	3.49	3.21	-4.26	-5.10	0.84	-3.85	0.41
tolmetin	156 ³	2.21	2.79	-4.13	-3.02	1.11	-3.41	0.72
tramadol	80	3.10	2.65	-2.24	-3.15	0.91	-3.27	1.03
verapamil	< 25	4.47	3.98	-3.97	-3.97	0.00	-4.64	0.67

Compound	MP (°C)	ClogP ^e	Observed logP	Observed logS ₀	logS _{GSE}	Absolute Error	logS _{Box&Comer}	Absolute Error
warfarin	161	2.89	3.54	-4.77	-3.75	1.02	-4.19	0.58
bendroflumethiazide	222	1.69	1.95	-4.33	-3.16	1.17	-2.55	1.78
benzthiazide	232	2.13	1.73	-4.83	-3.70	1.14	-2.32	2.51
ciprofloxacin	256 ³	-1.17	-1.08	-3.60	-0.64	2.96	0.57	4.17
famotidine	164	0.26	-0.81	-2.66	-1.15	1.52	0.29	2.95
flumequine	255	2.73	1.72	-3.88	-4.53	0.65	-2.31	1.57
folic acid	250 ³	-2.17	0.20	-5.31	0.42	5.73	-0.75	4.56
glipizide	209	2.53	2.58	-5.49	-3.87	1.63	-3.20	2.29
hydrochlorothiazide	274	-0.40	-0.07	-2.68	-1.59	1.09	-0.47	2.21
loperamide	228	4.68	4.87	-7.13	-6.21	0.92	-5.56	1.57
nitrofurantoin	263 ³	-0.47	-0.54	-3.33	-1.41	1.92	0.02	3.35
norfloxacin	228	-0.99	-1.03	-2.75	-0.54	2.22	0.52	3.27
piroxicam	199	1.89	1.98	-4.75	-3.13	1.62	-2.58	2.17
sulfamerazine	236	0.57	0.15	-3.10	-2.18	0.92	-0.69	2.41
sulfasalazine	220 ³	3.83	3.61	-6.28	-5.28	1.00	-4.26	2.02
sulfathiazole	189	0.72	0.07	-2.70	-1.86	0.84	-0.61	2.09
terfenadine	147	6.09	5.42	-7.74	-6.81	0.93	-6.12	1.62
tetracycline	173 ³	-0.91	-1.40	-3.09	-0.07	3.03	0.90	3.99
trichlormethiazide	270 ³	0.85	0.97	-3.41	-2.80	0.61	-1.54	1.87
4-iodophenol	94	2.89	2.91	-1.72	-3.08	1.36	-3.54	1.82
thymol	52	3.20	3.30	-2.19	-2.97	0.78	-3.94	1.75
chloroquine	< 25 ^{2,d}	5.05	4.99	-3.89	-4.55	0.66	-5.68	1.79

Compound	MP (°C)	ClogP ^e	Observed logP	Observed logS ₀	logS _{GSE}	Absolute Error	logS _{Box&Comer}	Absolute Error
quinacrine	87 ^{2, a}	6.71	5.44	-4.35	-6.83	2.48	-6.15	1.80
Average Absolute Error (n=81)						0.78		1.20

¹ The MP for alprenolol reported by Box and Comer of 108°C is the HCl salt, thus it is not valid with the GSE

² No MP was reported by Box and Comer

³ Decomposition temperature

⁴ Box and Comer reported a MP for miconazole of 161°C. The Merck Index (13th ed.) reports melting temperatures from 135-185°C for different forms of the nitrate salt. The 161°C is believed to be the nitrate salt, thus it is not valid with the GSE. No MP data could be found for the free base.

^a MP obtained from American Chemical Society. SciFinder Scholar, 2006.

^b MP obtained from United States Environmental Protection Agency 2000-2007. Estimation Programs Interface (EPI) Suite. 3.20.

^c Chaudhuri, N.K. and Ball, T.J. Synthesis of imipramine labelled with four deuterium atoms in 10, 11 positions. *Journal of Labelled Compounds and Radiopharmaceuticals*, **1980**, 25(8), 1189-1196.

^d Blauer, G.; Akkawi, M.; Fleischhacker, W.; Hiessbock, R. Synthesis and Optical Properties of the Chloroquine Enantiomers and Their Complexes With Ferriprotoporphyrin IX in Aqueous Solution. *Chirality*, **1998**, 10, 556-563.

^e Biobyte Corp 1995-1999. ClogP for Windows. 4.0.

The Box and Comer calculation yielded 45 drugs with errors greater than 1.0 log unit, whereas the GSE yielded only 19. Of the latter, 4 drugs are zwitterions for which the GSE is not applicable, and 6 drugs have only decomposition temperatures, which may be lower than the true melting point. Overall, with the additional crystallinity term, the GSE gives more accurate solubility predictions than predictions made by Box and Comer's equation.

A number of workers have used a single parameter to solve the problem of accurately predicting solubility. Log K_{ow} has been found to be the most useful of these; however, log K_{ow} alone is only half of the solution. By taking into account the crystal energy term, as reflected by the melting point, the GSE is able to predict more accurate solubility values for most of the compounds studied. This analysis shows that, with a minimum of input data, the GSE is more accurate in predicting the aqueous solubility of a wide variety of nonionized organic compounds. The GSE can be used without modification as it does not require a training set and does not include any fitted parameters.

Box and Comer³ determined supersaturation ratios for the compounds studied (*i.e.*, the kinetic solubility divided by the intrinsic solubility). They observed that the non-supersaturating drugs fall in a region of higher solubility, while most of the compounds that are highly supersaturated fall in the low solubility region of their plot. Their data show that the 10 non-supersaturating drugs with supersaturation ratios less than or equal

to 1.00 have melting temperatures less than 80°C. Also, 22 out of 26 drugs (85%) having supersaturation ratios of 1.5 or less, have melting points less than 100°C. In general, the melting point is indicative of the strength of the crystal lattice interactions. Low melting temperatures tell us that the solute molecules are weakly bound to one another and thus tend to have higher solubilities.

On the other hand, high melting temperatures suggest strong intermolecular interactions of the crystal, hence, lower aqueous solubilities and the tendency for greater supersaturation. Box and Comer's³ data also show that 24 of the 25 drugs (96%) with supersaturation ratios greater than 5.0 have melting points greater than 100°C (the 25th drug, chlorprothixene, has a melting temperature of 98°C). In addition, 21 of these 25 drugs (84%) have melting points greater than 150°C. The incidence of the vast majority of the supersaturated drugs having high melting temperatures illustrates, again, the role of the crystal term in predicting solubility.

5.4 Conclusion

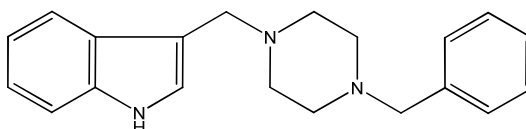
One of the most exploited physicochemical properties of a compound is its aqueous solubility and it is extremely relevant throughout all stages of the drug discovery and development process. When experimentally measured solubility data are not available, estimated or calculated values become very useful. The General Solubility Equation provides reasonably accurate solubility predictions of a wide variety of organic

compounds. It is derived from basic principles and it accounts for the crystal lattice energy of a solid solute as well as its aqueous activity coefficient. The GSE is simple to use as it only requires the compound's melting point and its octanol-water partition coefficient as input parameters, and it does not rely on a training set or regression-generated coefficients.

CHAPTER 6:
PREFORMULATION STUDY OF
3-[(4-BENZYLPIPERAZINO)METHYL]-1H-INDOLE (UA8967)

6.1 Introduction

3-[(4-benzylpiperazino)methyl]-1H-indole (UA8967) is a sparingly soluble, non-polar, basic compound that is being investigated for the treatment of pancreatic cancer, which remains the fourth leading cause of cancer death in the United States.^{1,2} Given the recent advances in the understanding of the disease on the molecular level, researchers are targeting specific genes for therapeutic development, such as the *deleted in pancreatic carcinoma locus 4 (DPC4)* gene which functions in the TGF-beta/ SMAD4 signaling pathway.³ Studies suggest that deletions or mutations in the tumor suppressor gene DPC4 are common in pancreatic cancer.^{1,4} Currently, researchers are investigating this novel agent, UA8967, which selectively targets pancreatic cancer cells with inactivated DPC4 (Dorr *in prep*).



3-[(4-benzylpiperazino)methyl]-1H-indole (UA8967)

In support of preclinical pharmacokinetic screening studies, physicochemical characterization and preformulation studies of UA8967 were conducted and the results are presented.

6.2 Methods

6.2.1 Reagents

UA8967 was purchased from Maybridge and used without further purification. The hydroxypropyl- β -cyclodextrin (HP β CD) (Cavasol W7 HP $\text{\textcircled{R}}$) used was supplied by Wacker and the Sulfobutyl Ether- β -cyclodextrin, sodium salt (SBE β CD) (Captisol $\text{\textcircled{R}}$) was supplied by CyDex, Inc. Hydrochloric acid and sodium hydroxide solutions used for pH adjustment were purchased from Aldrich. Sodium Chloride (Fisher), monobasic sodium phosphate (NaH_2PO_4 , Sigma), and dibasic sodium phosphate (Na_2HPO_4 , Sigma), were used to prepare phosphate buffered saline (PBS), pH 7.4 solutions.

6.2.2 Apparatus

The solubility of UA8967 was determined by reverse-phase HPLC with UV absorbance detection at 286 nm (Agilent Technology). Samples were eluted on a ZORBAX Eclipse XDB-C8 column (4.6 x 150 mm, 5 μm , Agilent) using a flow rate of 1.0 ml/min, an injection volume of 20 μl and a mobile phase composition of 68% Methanol and 32% Glycine/NaOH (Sorensen) buffer (0.05 M at pH 9).

pH measurements were performed using an Accumet AR15 pH meter which was calibrated using pH 2.00, 7.00, and 10.00 standard buffer solutions (VWR).

6.2.3 pH-Solubility and Stability Determination

Excess drug was added to 4 ml vials containing various buffer solutions. Sodium Citrate/HCl (Sorensen) and Glycine/HCl (Sorensen) were used to prepare pH 2-4 buffers. Phosphate (Sorensen) was used to prepare pH 5-8 buffers and Glycine/NaOH (Sorensen) was used for pH 9 and 10. All samples were set on an end-over-end mechanical rotator for equilibration. Due to the drug's poor chemical stability at low pH, the pH 2 saturated solutions were filtered and diluted with mobile phase after less than 10 minutes of equilibration. Similarly, saturated samples at pH 3 and 4 were filtered and assayed within 1-2 hours of equilibration. pH 5 samples were equilibrated for 24 hours and pH 6-10 samples were equilibrated for 48 hours. Sample pH was measured prior to filtering the saturated solution through 0.2 μm PTFE Acrodisc syringe filter. The supernatant was diluted in mobile phase and subsequently analyzed by HPLC.

pH stability studies at 25°C and 5°C were conducted on sample concentrations that were less than solubility at pH 3, 5 and 7. The buffers used for each pH are described in the reagents section above. Samples were filtered and analyzed by HPLC at various time points.

6.2.4 Equilibrium Cyclodextrin Solubility and Stability Determination

Drug-cyclodextrin complexes were prepared by adding excess drug to vials containing 1-2 ml solution of either HP β CD or SBE β CD at various concentrations ranging from 0-40% in PBS pH ~ 7.4. Samples were set on an end-over-end mechanical rotator to allow for equilibration up to 1 month. At various time points, saturated samples were filtered using a 0.2 μ m PTFE Acrodisc syringe filter and analyzed by HPLC.

Stability studies of the drug in 40% HP β CD or 40% SBE β CD at pH 3, 5, and 7 were conducted on sample concentrations below solubility. The various buffers used are described above in the reagents section. Samples were filtered and analyzed by HPLC at various time points.

6.2.5 Supersaturated Solution Preparation and Stability

A suspension sample was prepared by adding 10 - 20 mg of drug to 1 mL of vehicle (20% HP β CD or 20% SBE β CD in PBS, pH ~ 7.4). HCl gas was slowly bubbled into the suspension using a bulb attached to a glass Pasteur pipette. HCl gas was added until the sample became a clear solution and no solid particles were visible. The samples were vortexed periodically to facilitate dissolution and the resulting solution pH was between 1-2. The solution was immediately neutralized to approximately pH ~7.4 using 1N NaOH (Aldrich) to produce a clear supersaturated solution. Samples were set on an end-over-end mechanical rotator to allow for equilibration for up to 1 month. Additional samples

were stored at 5°C. At various time points, samples were filtered using a 0.2 µm PTFE Acrodisc syringe filter and analyzed by HPLC.

6.3 Results

6.3.1 pH-Solubility

Figure 6.1 shows the experimental pH-solubility data [●] for UA8967. The theoretical curves [solid lines] are calculated from the Henderson-Hasselbalch equation. The experimental data are consistent with the two curves described by Equations 1 and 2, and Table 6.1:

$$\log(S_{total} (\mu\text{g} / \text{ml})) = 1.76 \cdot (1 + 10^{8.58 - \text{pH}}) \quad (1)$$

$$\log(S_{total} (\mu\text{g} / \text{ml})) = 1139 \cdot (1 + 10^{3.35 - \text{pH}}) \quad (2)$$

Table 6.1. Experimental Intrinsic Aqueous Solubility, Solubility Product, and Dissociation Constants of UA8967

Intrinsic Aqueous Solubility S_w^{int} :	1.76 µg/ml
Solubility Product K_{sp} :	1139 µg/ml
Equilibrium constant pK_{a1} :	8.58
Equilibrium constant pK_{a2} :	3.35

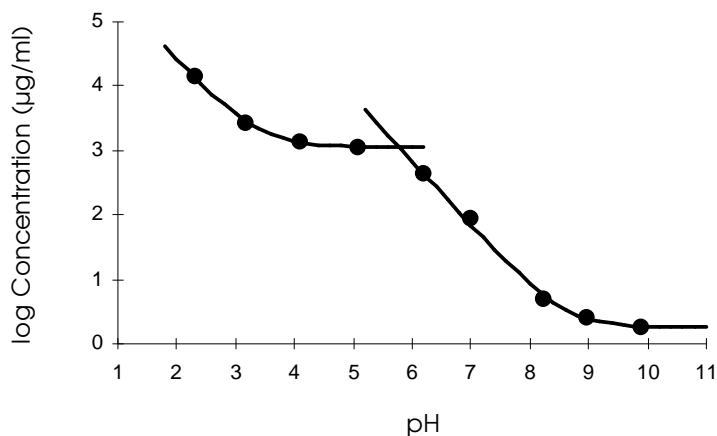


Figure 6.1. pH-Solubility profile of UA8967. Experimental data [●]. Henderson-Hasselbalch derived theoretical curve [solid line]

As a matter of convenience, the two solubility equations were independently calculated. The weakly basic drug is practically insoluble at high pH with an intrinsic water solubility of 1.8 µg/ml. At pH values below its first pka of 8.6, the solubility increases about 1000-fold but is limited by its solubility product. Further decreases in pH leads to the second ionization constant at 3.4 and an even greater increase in solubility to as much as 15 mg/ml at around pH 2.3.

6.3.2 pH-Stability in Aqueous and Cyclodextrin Solutions

Table 6.2 summarizes the experimental pH-stability data for UA8967 in various buffered solutions with and without cyclodextrin. UA8967 undergoes apparent first-order degradation. The degradation rates (k) were calculated from the slope of the linear regression line for the relationship between logarithm concentration versus time. The

drug is unstable in aqueous solutions with and without cyclodextrins at low pH (pH < 5). In buffer solutions without cyclodextrins, the half-life (T_{50}) is 7 hours at pH 3, 25°C. On the other hand, the drug is quite stable in aqueous solutions with and without cyclodextrins under neutral and basic conditions (pH > 7). At pH 7, 25°C, the half-life for the aqueous solution is over 2 months, and with 40% SBE β CD, up to 13 months. The solutions are more stable under 5°C at all pH conditions studied.

Table 6.2. pH Stability of UA8967 in Aqueous Solutions With and Without Cyclodextrins at 25°C and 5°C

Sample	1 st order degradation rate constant k (hour ⁻¹)		T ₉₀ (Days)		T ₅₀ (Days)	
	25°C	5°C	25°C	5°C	25°C	5°C
pH 3, buffer	0.09327	0.00345	0.05	1	0.3	8
pH 3, 40% HP β CD	0.00691	0.00023	0.6	19	4	125
pH 3, 40% SBE β CD	0.00921	0.00023	0.5	19	3	125
pH 5, buffer	0.00852	0.00023	0.5	19	3.4	125
pH 5, 40% HP β CD	0.00023	0.00005	19	95	125	627
pH 5, 40% SBE β CD	0.00069	0.00005	6	95	42	627
pH 7, buffer	0.00023	0.00002	19	272	125	1792
pH 7, 40% HP β CD	0.00018	0.00001	24	318	157	2091
pH 7, 40% SBE β CD	0.00007	0.00001	24	381	418	2509

The pH stability data in pH 3 and pH 7 aqueous and cyclodextrin solutions at 25°C and 5°C, are graphically displayed in Figures 6.2 and 6.3. The data in Figure 6.2 show the room temperature stability at pH 3 is significantly greater in the two cyclodextrin solutions (---■--- and ---●---) than in the buffer alone (---▲---). Clearly, the stability at 5°C (solid lines) is much improved over 25°C (dotted lines) for aqueous and cyclodextrin solutions, with the cyclodextrins producing a definite protective effect. It is clear in Figure 6.3, that the stability of UA8967 at pH 7 is nearly identical in both buffer solution and in 40% cyclodextrin solutions. Furthermore, very little difference in the degradation rate exists between 25°C and 5°C.

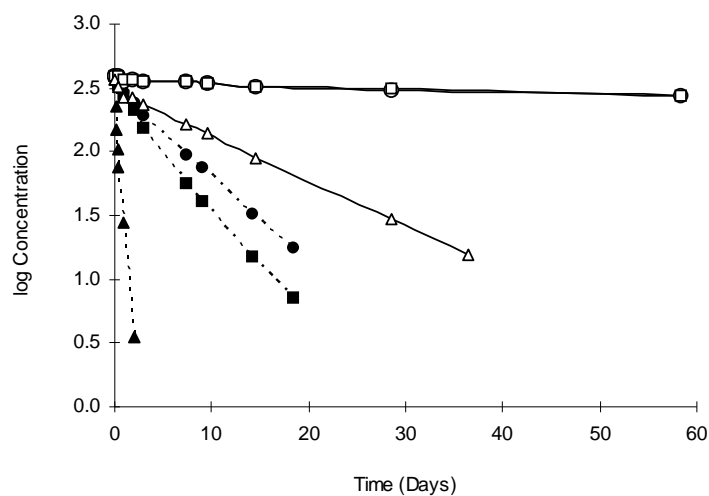


Figure 6.2. pH-stability data in aqueous and 40% cyclodextrin solutions at pH 3. Aqueous solution at 25°C (---▲---) and at 5°C (—△—). 40% HPβCD at 25°C (---●---) and at 5°C (—○—). 40% SBEβCD at 25°C (---■---) and at 5°C (—□—).

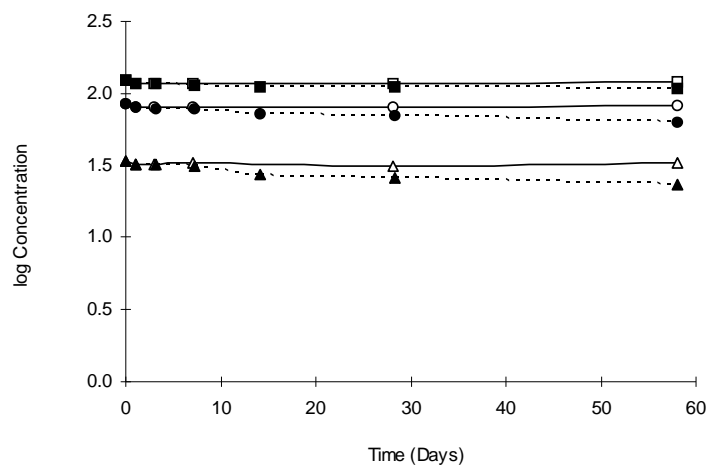


Figure 6.3. pH-stability data in aqueous and 40% cyclodextrin solutions at pH 7. Aqueous solution at 25°C (---▲---) and at 5°C (—△—). 40% HPβCD at 25°C (---●---) and at 5°C (—○—). 40% SBEβCD at 25°C (---■---) and at 5°C (—□—).

6.3.3 Cyclodextrin Solubility

The solubility of UA8967 near physiological pH conditions as a function of concentrations of HPβCD and SBEβCD in PBS is illustrated in Figure 6.4. At pH ~7.6, the drug predominantly (~91%) exists in an ionized state. Both curves in Figure 6.4 describe a linear increase in solubility with concentration and suggests that a 1:1 (Drug:HPβCD and Drug:SBEβCD) complex is formed. At pH 7.6, the effective stability constant for a 1:1 complexation with HPβCD is 349 M^{-1} and 477 M^{-1} with SBEβCD. Although the slopes of the two lines in Figure 6.4 are very similar (0.12 for HPβCD and 0.11 for SBEβCD), on a mole basis, the latter has the higher solubilization capacity, given its average molecular weight of 2146 g/mol, as compared to 1399 g/mol for HPβCD. In the absence of cyclodextrin, the solubility at pH 7.6 is $5.8 \text{ } \mu\text{g/ml}$ and

increases by nearly 3 orders of magnitude in cyclodextrin, up to 5.3 mg/ml in 40% HP β CD and 4.5 mg/ml in 40% SBE β CD.

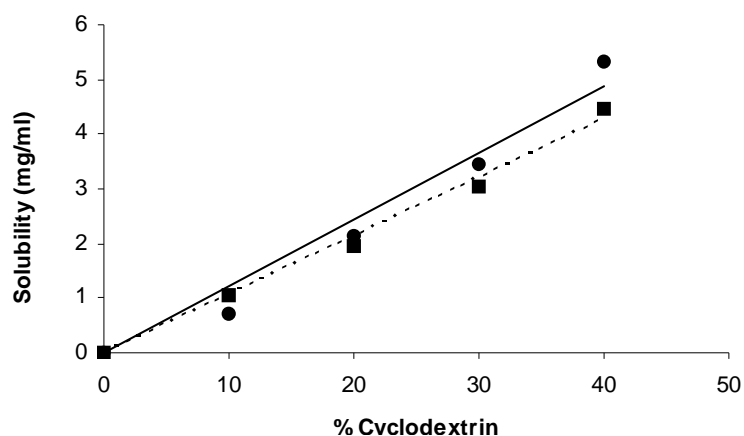


Figure 6.4. Solubility of UA8967 as a function of cyclodextrin concentration in phosphate buffer saline, pH ~ 7.6. HP β CD (●) and SBE β CD (■).

6.3.4 Supersaturated Formulations

Supersaturated solutions were successfully prepared at about 10 mg/ml in 20% HP β CD and 20% SBE β CD in PBS, pH ~ 7.4. In terms of physical stability, samples were visually inspected for precipitation on each day they were assayed. Each sample, whether or not it was clear, was filtered with a 0.2 μ m PTFE Acrodisc syringe filter prior to sample analysis. The 20% HP β CD supersaturated samples remain free of precipitate for up to 31 days at 25°C and 5°C. The 20% SBE β CD samples are physically stable up to 5 days at 25°C and for at least 31 days at 5°C. Figure 6.5 shows the kinetics of the

metastable supersaturated solutions (top 4 curves) for the 25°C (dotted lines) and 5°C (solid lines) samples. The drug loss over time for each sample, except the 25°C 20% SBE β CD, is due to chemical degradation, not the conversion of the metastable solution to a more thermodynamically stable one. The 20% SBE β CD solution at 25°C, on the other hand, did precipitate within 5 days and maintained a lower but relatively constant supersaturated concentration up to one month. For comparison, a plot of the equilibrium solubility of the drug in 20% HP β CD and 20% SBE β CD PBS solutions at 25°C (dotted lines) are also included. These solutions (bottom 2 curves) reach equilibrium within 1 day.

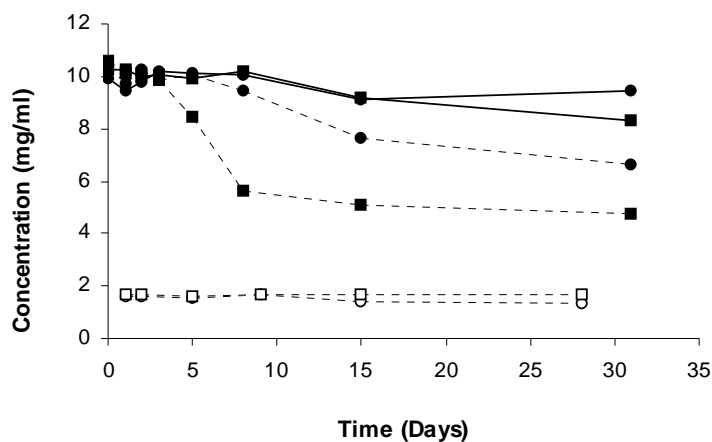


Figure 6.5. Equilibrium and supersaturated solutions of UA8967 in 20% cyclodextrin PBS solutions at 25°C and 5°C. Equilibrium solution of 20% HP β CD at 25°C (--- \square ---) and 20% SBE β CD at 25°C (--- \square ---). Supersaturated solution of 20% HP β CD at 25°C (--- \bullet ---) and 20% SBE β CD at 25°C (--- \blacksquare ---). Supersaturated solution of 20% HP β CD at 5°C (— \bullet —) and 20% SBE β CD at 5°C (— \blacksquare —).

6.4 Discussion

6.4.1 Physicochemical Properties

The physicochemical characteristics of UA8967 present a challenge in preparing a suitable preclinical solution formulation at a relatively high dose. The compound is a non-polar sparingly soluble basic drug with a molecular weight of 305.42 g/mol, an intrinsic aqueous solubility of 1.8 $\mu\text{g/ml}$, and a calculated $\log P^5$ of 4.16. Experimental pKa values were determined to be approximately 3.4 and 8.6 and the compound's melting point is 168°C.

6.4.2 Cosolvent Solubilization

None of the common pharmaceutically acceptable solvents such as ethanol, propylene glycol, and PEG 400, provide the needed solubility, even at 100% cosolvent concentration. Although the drug is highly soluble in 100% DMA and 100% NMP, the use of these cosolvents is precluded by the fact that the drug precipitates at a 1 to 10 and 1 to 100 dilution in water.

6.4.3 pH-Solubility and Stability

Given the two ionizable nitrogens present in the molecule, pH-solubility enhancement is an obvious strategy to explore. Since the acceptable pH range of an IV or IP formulation is pH 3-9, a pH-solubility profile was conducted from pH 2 to 10. The data in Figure 6.1 suggest that a solubility product is reached between the two dissociation constants

resulting in the second pH-solubility curve. Unfortunately, the water solubility of UA8967 at pH 3 (2.76 mg/ml) does not provide a high enough concentration to meet the desired dose. The pH-solubility profile shows that the drug can reach concentrations greater than 15 mg/ml only at pH values that are not acceptable for parenteral delivery. Not only are there pH restrictions to consider, but as Table 6.1 and Figure 6.2 show, the drug is unstable at low pH (T_{50} of 7 hours at pH 3). Consequently, a buffered solution at low pH is not a viable formulation approach.

6.4.4 Cyclodextrin Solubilization and Stabilization

The solubilization of poorly water-soluble drugs by cyclodextrin complexation has been extensively studied.⁶⁻¹¹ Cyclodextrins are cyclic oligosaccharides consisting of 6, 7, and 8 units of glucose (α -CD, β -CD, and γ -CD) joined by α -1,4 bonds. The internal diameter of α -CD is the smallest ($\sim 5\text{\AA}$), while β -CD and γ -CD are larger (approx. 6\AA and 8\AA , respectively).¹² The interior cavity is relatively hydrophobic due to the CH_2 and ether groups, whereas the exterior, consisting of primary and secondary hydroxyl groups, is more polar. Water inside the cavity tends to get replaced by more nonpolar molecules. The ability of cyclodextrins to form noncovalent inclusion complexes with molecules that partially fit inside its nonpolar cavity leads to drug solubilization. Two water-soluble β -CD derivatives of pharmaceutical interest are hydroxypropyl β -cyclodextrin (HP β CD) and sulfobutyl ether β -cyclodextrin (SBE β CD), both of which have been shown to be safe and well tolerated.

Aqueous formulations using SBE β CD have proven to be successful in at least two commercially available injectable formulations, Vfend and Geodeon. From our studies however (Figure 4), UA8967's solubility in various concentrations of HP β CD and SBE β CD in PBS, pH \sim 7.4, only reaches 5.3 mg/ml in 40% HP β CD. Although the cyclodextrins indeed improve the water solubility of the drug by nearly 1000-fold, this is not sufficient for an aqueous formulation.

For ionizable drugs, the effect of complexation and pH control on solubilization is well understood.^{6, 8, 9, 13, 14} In general, the stability constant for the free acid or free base is significantly larger than the stability constant of its salt. On the other hand, the aqueous solubility of the ionized species is greater than that of the unionized form. Depending on which effect is greater on solubility - ionization or complexation - the total solubility of a solute can be optimized by the combined effect of pH and cyclodextrin complexation.

Although the most common pharmaceutical application of cyclodextrins is to enhance aqueous solubility,^{6, 7, 9, 11} inclusion complexation can also lend a hand in stabilization of chemically labile drugs. Depending on the type of reaction and the orientation of the solute in the CD cavity, cyclodextrins may retard or accelerate drug degradation.

Numerous studies of the effect of cyclodextrins on drug stability have been reported.^{6, 15-}

As already mentioned, the chemical stability of UA8967 is highly dependent on pH. Figure 6.2 shows that inclusion complexation with cyclodextrin provides a protective effect against chemical degradation resulting in more stable solutions. This effect is clearly seen at low pH, where the drug is extremely unstable. It is 10 times more stable in 40% cyclodextrin than in water at pH 3 at room temperature. At the relatively stable condition of pH 7, complexation with HP β CD and SBE β CD improves the solution stability about 2 and 4 times, respectively.

6.4.5 Clear and Stable Supersaturated Solutions

By taking advantage of the fact that, cyclodextrins provide protection from chemical degradation as well as retard precipitation, while pH control facilitates dissolution and solubility, two suitable preclinical supersaturated solution formulations were successfully developed. Drug concentrations exceeding 10 mg/ml were obtained by temporarily adjusting the pH of the cyclodextrin solution to below 2 so that the inclusion process can occur. Since the solution is not exposed to the acidic environment for more than a few minutes, solute stability is not significantly compromised. The solution is subsequently neutralized to pH \sim 7.4 producing a clear and stable supersaturated formulation. This is at least a 100-fold increase in concentration over the aqueous solubility of 70 μ g/ml.

In terms of the physical stability (*i.e.*, no precipitate), Figure 6.5 shows that the hydroxypropyl beta-cyclodextrin provides a more physically stable complex with the drug than the sulfobutyl ether beta-cyclodextrin, particularly at 25°C. A 10 mg/ml

supersaturated formulation in 20% HP β CD at room temperature is free of precipitate for a longer period of time than in 20% SBE β CD (up to 31 days and 5 days, respectively). When stored at 5°C, the supersaturated formulation in both cyclodextrins solution remain clear for up to a month. This is likely due to the fact that the drug is poorly soluble in water at 5°C and therefore tends to preferentially remain in the cyclodextrin cavity. Also, the addition of 10% (w/v) PVP K12 to a 20% SBE β CD pH ~7.4 supersaturated system (data not included), resulted in a clear and physically stable solution for at least 7 weeks at 5°C. Water soluble polymers have been reported to retard the crystal growth²⁰ of supersaturated solutions, as well as, to increase the stability constants of drug-cyclodextrin complexes.^{21, 22} For long term chemical and physical stability, the ability to lyophilize the formulation for reconstitution will be investigated.

6.5 Conclusion

pH adjustment or complexation alone of this poorly water soluble basic drug did not provide an acceptable formulation. Furthermore, UA8967 is highly susceptible to acid catalyzed hydrolysis. However, cyclodextrin complexation in combination with pH enabled the successful formulation of a supersaturated solution. pH control produced an increase in the dissolution rate and solubilization of the solute for inclusion into the β -cyclodextrin cavity, while inclusion complexation provided a stabilizing effect. Neutralization of the formulation subsequently led to a stable supersaturated solution at

physiological pH. The formulation is clear and stable for 31 days at both room temperature and refrigerated conditions.

REFERENCES

References for Chapter 1

1. Herper, M. Drug Drought. *Forbes.com* **2007**.
2. Tufts Center for the Study of Drug Development Backgrounder: A Methodology for Counting Costs for Pharmaceutical R&D. **2001**.
3. Kola, I.; Landis, J. Can the pharmaceutical industry reduce attrition rates? *Nature Reviews* **2004**, *3*, 711-715.
4. Oprea, T. I. Current trends in lead discovery: Are we looking for the appropriate properties? *Journal of Computer-Aided Molecular Design* **2002**, *16*, 325--334.
5. Balani, S. K.; Miwa, G. T.; Gan, L.; Wu, J.; Lee, F. W. Strategy of utilizing in vitro and in vivo ADME tools for lead optimization and drug candidate selection. *Current Topics in Medicinal Chemistry* **2005**, *5*, 1033-1038.
6. Eddershaw, P. J.; Beresford, A. P.; Bayliss, M. K. ADME/PK as part of a rational approach to drug discovery. *Drug Discovery Today* **2000**, *5*, 409-414.
7. Gombar, V. K.; Silver, I. S.; Zhao, Z. Role of ADME characteristics in drug discovery and their in silico evaluation: In silico screening of chemicals for their metabolic stability. *Current Topics in Medicinal Chemistry* **2003**, *3*, 1205-1225.
8. Kassel, D. B. Applications of high-throughput ADME in drug discovery. *Current Opinion in Chemical Biology* **2004**, *8*, 339-345.
9. van de Waterbeemd, H.; Gifford, E. ADMET In Silico Modelling. Towards Prediction Paradise? *Nature* **2003**, *2*, 192-204.
10. Wenlock, M. C.; Austin, Rupert P.; Barton, Patrick; Davis, A. M.; Leeson, P. D. A Comparison of Physiochemical Property Profiles of Development and Marketed Oral Drugs. *Journal of Medicinal Chemistry* **2003**, *46*, 1250--1256.
11. Lipinski, C. A.; Lombardo, F.; Dominy, B. W.; Feeney, P. J. Experimental and computational approaches to estimate solubility and permeability in drug discovery and development settings. *Advanced Drug Delivery Reviews* **1997**, *23*, 3--25.

12. Sakaeda, T.; Okamura, N.; Nagata, S.; Yagami, T.; Horinouchi, M.; Okumura, K.; Yamashita, F.; Hashida, M. Molecular and Pharmacokinetic Properties of 222 Commercially Available Oral Drugs in Humans. *Biol. Pharm. Bull.* **2001**, *24*, 935--940.
13. Horter, D.; Dressman, J. B. Influence of physicochemical properties on dissolution of drugs in the gastrointestinal tract. *Advanced Drug Delivery Reviews* **2001**, *46*, 78-87.
14. Welling, P. G. Effects of food on drug absorption. *Annual Review of Nutrition* **1996**, *16*, 383-415.
15. Cummins, C. L.; Mangravite, L. M.; Benet, L. Z. Characterizing the Expression of CYP3A4 and Efflux Transporters (P-gp, MRP1, and MRP2) in CYP3A4-Transfected Caco-2 Cells After Induction with Sodium Butyrate and the Phorbol Ester 12-O-Tetradecanoylphorbol-13-Acetate. *Pharmaceutical Research* **2001**, *18*, 1102-1109.
16. Cummins, C. L.; Jacobsen, W.; Benet, L. Z. Unmasking the Dynamic Interplay between Intestinal P-Glycoprotein and CYP3A4. *The Journal of Pharmacology and Experimental Therapeutics* **2002**, *300*, 1036-1045.
17. Kolars, J. C.; Awni, W. M.; Merion, R. M.; Watkins, P. B. First-pass metabolism of cyclosporin by the gut. *The Lancet* **1991**, *338*, 1488-1490.
18. Thummel, K. E.; O'Shea, D.; Paine, M. F.; Shen, D. D.; Kunze, K. L.; Perkins, J. D.; Wilkinson, G. R. Oral first-pass elimination of midazolam involves both gastrointestinal and hepatic CYP3A-mediated metabolism. *Clinical Pharmacology and Therapeutics* **1996**, *59*, 491-502.
19. Zhang, Y.; Benet, L. Z. The Gut as a Barrier to Drug Absorption. Combined Role of Cytochrome P450 3A and P-Glycoprotein. *Clinical Pharmacokinetics* **2001**, *40*, 159-168.
20. Stenberg, P.; Norinder, U.; Luthman, K.; Artursson, P. Experimental and computational screening methods for the prediction of intestinal drug absorption. *Journal of Medicinal Chemistry* **2001**, *44*, 1927-1937.
21. van de Waterbeemd, H.; Camenisch, G.; Folkers, G.; Raevsky, O. A. Estimation of Caco-2 Cell Permeability Using Calculated Molecular Descriptors. *QSAR & Combinatorial Science* **1996**, *15*, 480-490.
22. Hansch, C.; Quinlan, J. E.; and Lawrence, G. L. The linear free-energy relationship between partition coefficients and the aqueous solubility of organic liquids. *The Journal of Organic Chemistry* **1968**, *33*, 347-350.

23. Yalkowsky, S. H. In *Solubility and Solubilization in Aqueous Media*. ACS/Oxford University Press: New York, New York, 2010; .
24. Jain, N.; Yalkowsky, S. H. Estimation of the aqueous solubility I: Application to organic nonelectrolytes. *Journal of Pharmaceutical Sciences* **2001**, *90*, 234--252.

References for Chapter 2

1. van de Waterbeemd, H.; Camenisch, G.; Folkers, G.; Raevsky, O. A. Estimation of Caco-2 Cell Permeability Using Calculated Molecular Descriptors. *QSAR & Combinatorial Science* **1996**, *15*, 480-490.
2. Palm, K.; Luthman, K.; Ros, J.; Grasjo, J.; Artursson, P. Effect of molecular charge on intestinal epithelial drug transport: pH dependent transport of cationic drugs. *The Journal of Pharmacology and Experimental Therapeutics* **1999**, *291*, 435-443.
3. Agatonovic-Kustrin, S.; Beresford, R.; Yusof, A. P. M. Theoretically derived molecular descriptors important in human intestinal absorption. *Journal of Pharmaceutical and Biomedical Analysis* **2001**, *25*, 227-237.
4. Clark, D. E.; Pickett, S. D. Computational methods for the prediction of 'drug-likeness'. *Drug Discovery Today* **2000**, *5*, 49-57.
5. Palm, K.; Luthman, K.; Ungell, A.; Strandlund, G.; Artursson, P. Correlation of drug absorption with molecular surface properties. *Journal of Pharmaceutical Sciences* **1996**, *85*, 32-39.
6. Stenberg, P.; Norinder, U.; Luthman, K.; Artursson, P. Experimental and computational screening methods for the prediction of intestinal drug absorption. *Journal of Medicinal Chemistry* **2001**, *44*, 1927-1937.
7. van de Waterbeemd, H.; Gifford, E. ADMET In Silico Modelling. Towards Prediction Paradise? *Nature* **2003**, *2*, 192-204.
8. Palm, K.; Luthman, K.; Ungell, A.; Strandlund, G.; Beigi, F.; Lundahl, P.; Artursson, P. Evaluation of Dynamic Polar Molecular Surface Area as Predictor of Drug Absorption: Comparison with Other Computational and Experimental Predictors. *Journal of Medicinal Chemistry* **1998**, *41*, 5382-5392.
9. Biobyte Corp ClogP for Windows. **1995-1999**, *4.0*.
10. Advanced Chemistry Development Inc. ACD/Labs 7.0. , *7.09*.

11. Camenisch, G.; Folkers, G.; van de Waterbeemd, H. Review of theoretical passive drug absorption models: Historical background, recent developments and limitations. *Pharmaceutica Acta Helvetiae* **1996**, *71*, 309-327.
12. Palm, K.; Stenberg, P.; Luthman, K.; Artursson, P. Polar Molecular surface properties predict the intestinal absorption of drugs in humans. *Pharmaceutical Research* **1997**, *14*, 568-571.
13. Camenisch, G.; Alsenz, J.; van de Waterbeemd, H.; Folkers, G. Estimation of permeability by passive diffusion through Caco-2 cells using the drugs' lipophilicity and molecular weight. *European Journal of Pharmaceutical Sciences* **1998**, *6*, 313-319.
14. Conradi, R. A.; Hilgers, A. R.; Ho, N. F. H.; Burton, P. S. The influence of peptide structure on transport across Caco-2 cells. II. Peptide bond modification which results in improved permeability. *Pharmaceutical Research* **1992**, *9*, 435-439.
15. Clark, D. E. Rapid calculation of polar molecular surface area and its application to the prediction of transport phenomena. 1. Prediction of intestinal absorption. *Journal of Pharmaceutical Sciences* **1999**, *88*, 807-814.

References for Chapter 3

1. Palm, K.; Stenberg, P.; Luthman, K.; Artursson, P. Polar Molecular surface properties predict the intestinal absorption of drugs in humans. *Pharmaceutical Research* **1997**, *14*, 568-571.
2. Clark, D. E. Rapid calculation of polar molecular surface area and its application to the prediction of transport phenomena. 1. Prediction of intestinal absorption. *Journal of Pharmaceutical Sciences* **1999**, *88*, 807-814.
3. Zhao, Y. H.; LE, J.; Abraham, M. H.; Hersey, A.; Eddersshaw, P. J.; Luscombe, C. N.; Boutina, D.; Beck, G.; Sherborne, B.; Cooper, I. Evaluation of human intestinal absorption data and subsequent derivation of a quantitative structure-activity relationship (QSAR) with the Abraham descriptors. *Journal of Pharmaceutical Sciences* **2001**, *90*, 749--784.
4. Lipinski, C. A.; Lombardo, F.; Dominy, B. W.; Feeney, P. J. Experimental and computational approaches to estimate solubility and permeability in drug discovery and development settings. *Advanced Drug Delivery Reviews* **1997**, *23*, 3--25.

5. Stehle, R. G.; Higuchi, W. I. In Vitro Model for Transport of Solutes in Three-Phase System I: Theoretical Principles. *Journal of Pharmaceutical Sciences* **1972**, *61*, 1922--1930.
6. Stehle, R. G.; Higuchi, W. I. In Vitro Model for Transport of Solutes in Three-Phase System II: Experimental Considerations. *Journal of Pharmaceutical Sciences* **1972**, *61*, 1931--1935.
7. Flynn, G. L.; Yalkowsky, S. H. Correlation and Prediction of Mass Transport across Membranes I: Influence of Alkyl Chain Length on Flux-Determining Properties of Barrier and Diffusant. *Journal of Pharmaceutical Sciences* **1972**, *61*, 838--852.
8. Flynn, G. L.; Yalkowsky, S. H.; Roseman, T. J. Mass transport phenomena and models: Theoretical concepts. *Journal of Pharmaceutical Sciences* **1974**, *63*, 479-510.
9. Yalkowsky, S. H.; Carpenter, O. S.; Flynn, G. L.; Slunick, T. G. Drug Absorption Kinetics in Goldfish. *Journal of Pharmaceutical Sciences* **1973**, *62*, 1949--1954.
10. Yalkowsky, S. H.; Slunick, T. G.; Flynn, G. L. Effects of alkyl chain length on biological activity: Alkyl p-aminobenzoate-induced narcosis in goldfish. *Journal of Pharmaceutical Sciences* **1974**, *63*, 691-695.
11. Dressman, J. B.; Amidon, G. L.; Fleisher, D. Absorption Potential: Estimating the Fraction Absorbed for Orally Administered Compounds. *Journal of Pharmaceutical Sciences* **1985**, *74*, 588--589.
12. Balon, K.; Riebesehl, B. U.; Muller, B. W. Drug liposome partitioning as a tool for the prediction of human passive intestinal absorption. *Pharmaceutical Research* **1999**, *16*, 882--888.
13. Palm, K.; Luthman, K.; Ros, J.; Grasjo, J.; Artursson, P. Effect of molecular charge on intestinal epithelial drug transport: pH dependent transport of cationic drugs. *The Journal of Pharmacology and Experimental Therapeutics* **1999**, *291*, 435-443.
14. Johnson, K. C.; Swindell, A. C. Guidance in the setting of drug particle size specifications to minimize variability in absorption. *Pharmaceutical Research* **1996**, *13*, 1795--1798.
15. Sanghvi, T.; Ni, N.; Yalkowsky, S. H. A simple modified absorption potential. *Pharmaceutical Research* **2001**, *18*, 1794--1796.
16. Chu, K. A.; Yalkowsky, S. H. An interesting relationship between drug absorption and melting point. *International Journal of Pharmaceutics* **2009**, *373*, 24-40.

17. van de Waterbeemd, H.; Jones, B. C. Predicting Oral Absorption and Bioavailability. *Progress in Medicinal Chemistry* **2003**, *41*, 1--59.
18. Ni, N.; Sanghvi, T.; Yalkowsky, S. H. Independence of the product of solubility and distribution coefficient of pH. *Pharmaceutical Research* **2002**, *19*, 1862--1866.
19. Sanghvi, T.; Ni, N.; Mayersohn, M.; Yalkowsky, S. H. Predicting passive intestinal absorption using a single parameter. *QSAR Comb. Sci.* **2003**, *22*, 247--257.
20. Yalkowsky, S. H.; Johnson, J. L. H.; Sanghvi, T.; Machatha, S. G. A 'Rule of Unity' for human intestinal absorption. *Pharmaceutical Research* **2006**, *23*, 2475--2481.
21. Jain, N.; Yalkowsky, S. H. Estimation of the aqueous solubility I: Application to organic nonelectrolytes. *Journal of Pharmaceutical Sciences* **2001**, *90*, 234--252.
22. Thomas, V. H.; Bhattachar, S.; Hitchingham, L.; Zocharski, P.; Naath, M.; Surendran, N.; Stoner, L. C.; El-Kattan, A. The road map to oral bioavailability: an industrial perspective. *Expert Opinion on Drug Metabolism and Toxicology* **2006**, *2*, 4-591.
23. Advanced Chemistry Development Inc. ACD/Labs 7.0., 7.09 .

References for Chapter 4

1. Ajay; Walters, W. P.; Murcko, M. A. Can We Learn To Distinguish between "Drug-like" and "Nondrug-like" Molecules? *J. Med. Chem.* **1998**, *41*, 3314-3324.
2. Sadowski, J.; Kubinyi, H. A Scoring Scheme for Discriminating between Drugs and Nondrugs. *Journal of Medicinal Chemistry* **1998**, *41*, 3325--3329.
3. Oprea, T. I.; Davis, A. M.; Teague, S. J.; Leeson, P. D. Is there a difference between leads and drugs? A historical perspective. *J Chem Inf Comput Sci* **2001**, *41*, 1308--1315.
4. Biswas, D.; Roy, S.; Sen, S. A simple approach for indexing the oral druglikeness of a compound: Discriminating druglike compounds from nondruglike ones. *J Chem Inf Model* **2006**, *46*, 1394--1401.
5. Lipinski, C. A.; Lombardo, F.; Dominy, B. W.; Feeney, P. J. Experimental and computational approaches to estimate solubility and permeability in drug discovery and development settings. *Advanced Drug Delivery Reviews* **1997**, *23*, 3--25.

6. Amidon, G. L.; Lennernas, H.; Shah, V. P.; Crison, J. R. A theoretical basis for a biopharmaceutic drug classification: The correlation of in vitro drug product dissolution and in vivo bioavailability. *Pharmaceutical Research* **1995**, *12*, 413--420.
7. Dressman, J. B.; Amidon, G. L.; Fleisher, D. Absorption Potential: Estimating the Fraction Absorbed for Orally Administered Compounds. *Journal of Pharmaceutical Sciences* **1985**, *74*, 588--589.
8. Balon, K.; Riebesehl, B. U.; Muller, B. W. Drug liposome partitioning as a tool for the prediction of human passive intestinal absorption. *Pharmaceutical Research* **1999**, *16*, 882--888.
9. Sanghvi, T.; Ni, N.; Yalkowsky, S. H. A simple modified absorption potential. *Pharmaceutical Research* **2001**, *18*, 1794--1796.
10. Johnson, K. C.; Swindell, A. C. Guidance in the setting of drug particle size specifications to minimize variability in absorption. *Pharmaceutical Research* **1996**, *13*, 1795--1798.
11. Ni, N.; Sanghvi, T.; Yalkowsky, S. H. Independence of the product of solubility and distribution coefficient of pH. *Pharmaceutical Research* **2002**, *19*, 1862--1866.
12. Willmann, S.; Schmitt, W.; Keldenich, J.; Lippert, J.; Dressman, J. B. A physiological model for the estimation of the fraction dose absorbed in humans. *Journal of Medicinal Chemistry* **2004**, *47*, 4022--4031.
13. Sanghvi, T.; Ni, N.; Mayersohn, M.; Yalkowsky, S. H. Predicting passive intestinal absorption using a single parameter. *QSAR Comb. Sci.* **2003**, *22*, 247--257.
14. Jain, N.; Yalkowsky, S. H. Estimation of the aqueous solubility I: Application to organic nonelectrolytes. *Journal of Pharmaceutical Sciences* **2001**, *90*, 234--252.
15. Zhao, Y. H.; LE, J.; ABRAHAM, M. H.; Hersey, A.; Eddersshaw, P. J.; Luscombe, C. N.; Boutina, D.; Beck, G.; Sherborne, B.; Cooper, I. Evaluation of human intestinal absorption data and subsequent derivation of a quantitative structure-activity relationship (QSAR) with the Abraham descriptors. *Journal of Pharmaceutical Sciences* **2001**, *90*, 749--784.
16. MayoClinic.com Cephalosporin (Oral Route, Injection Route, Intravenous Route, Intramuscular Route). <http://www.mayoclinic.com/health/drug-information/DR600239>.
17. Kohda-Shimizu, R.; Li, Y.; Shitara, Y.; Ito, K.; Tsuda, Y.; Yamada, H.; Itoh, T. Oral absorption of cephalosporins is quantitatively predicted from in vitro uptake into

- intestinal brush border membrane vesicles. *International Journal of Pharmaceutics* **2001**, *220*, 119--128.
18. United States Environmental Protection Agency Estimation Programs Interface (EPI) Suite. **2000-2007**, *3.20*, .
 19. American Chemical Society SciFinder Scholar. **2005**, *2006*, .
 20. Yalkowsky, S. H., (Ed.) *AQUASOL dATABASE of aqueous solubility*. **1999**, .
 21. Merck Research Laboratories In *The Merck Index*. Whitehouse Station, NJ, 2001; .
 22. Biobyte Corp ClogP for Windows. **1995-1999**, *4.0*, .
 23. Curatolo, W. Physical chemical properties of oral drug candidates in the discovery and exploratory development settings. *Research Focus* **1998**, *1*, 387--393.

References for Chapter 5

1. Jain, N.; Yalkowsky, S. H. Estimation of the aqueous solubility I: Application to organic nonelectrolytes. *Journal of Pharmaceutical Sciences* **2001**, *90*, 234--252.
2. Jain, P.; Sepassi, K.; Yalkowsky, S. H. Comparison of aqueous solubility estimation for AQUAFAC and GSE. *International Journal of Pharmaceutics* **2008**, *360*, 122-147.
3. Box, K.J. and Comer, J.E. A Using measured pKa, logP and solubility to investigate supersaturation and predict BCS class. *Current Drug Metabolism* **2008**, *9*, 869-878.
4. Biobyte Corp ClogP for Windows. **1995-1999**, *4.0*, .
5. Hansch, C.; Quinlan, J. E.; and Lawrence, G. L. The linear free-energy relationship between partition coefficients and the aqueous solubility of organic liquids. *The Journal of Organic Chemistry* **1968**, *33*, 347-350.

References for Chapter 6

1. Jaffee, E. M.; Hruban, R. H.; Canto, M.; Kern, S. E. Focus on pancreas cancer. *Cancer Cell* **2002**, *2*, 25-28.

2. Jemal, A.; Murray, T.; Ward, E.; Samuels, A.; Tiwari, R. C.; Ghafoor, A.; Feuer, E. J.; Thun, M. J. Cancer statistics, 2005. *A Cancer Journal for Clinicians* **2005**, *55*, 10-30.
3. Jones, S.; Zhang, X.; Parsons, D. W.; *et al.* Core signaling pathways in human pancreatic cancers revealed by global genomic analyses. *Science* **2008**, *321*, 1801-1806.
4. Miyaki, M.; Kuroki, T. Role of Smad4 (DPC4) inactivation in human cancer. *Biochemical and Biophysical Research Communications* **2003**, *306*, 799-804.
5. Biobyte Corp ClogP for Windows. **1995-1999**, *4.0*.
6. Loftsson, T.; Brewster, M. E. Pharmaceutical Applications of Cyclodextrins. 1. Drug Solubilization and Stabilization. *Journal of Pharmaceutical Sciences* **1996**, *85*, 1017-1025.
7. Stella, V. J.; Rajewski, R. A. Cyclodextrins: Their future in drug formulation and delivery. *Pharmaceutical Research* **1997**, *14*, 556-567.
8. Li, P.; Tabibi, E.; Yalkowsky, S. H. Combined effect of complexation and pH on solubilization. *Journal of Pharmaceutical Sciences* **1998**, *87*, 1535-1537.
9. Xiang, T.; Anderson, B. D. Stable supersaturated aqueous solutions of Silatecan 7-t-Butyldimethylsilyl-10-Hydroxycamptothecin via chemical conversion in the presence of a chemically modified b-cyclodextrin. *Pharmaceutical Research* **2002**, *19*, 1215-1222.
10. Loftsson, T.; Hreinsdottir, D.; Masson, M. Evaluation of cyclodextrin solubilization of drugs. *International Journal of Pharmaceutics* **2005**, *302*, 18-28.
11. Brewster, M. E.; Loftsson, T. Cyclodextrins as pharmaceutical solubilizers. *Advanced Drug Delivery Reviews* **2007**, *59*, 645-666.
12. Martin, A.; Bustamante, P.; Chun, A. H. C. In *Physical Pharmacy*. Lippincott Williams and Wilkins: Baltimore, MD, 1993; pp 257-260.
13. McCandless, R.; Yalkowsky, S. H. Effect of hydroxypropyl-b-cyclodextrin and pH on the solubility of Levemopamil HCl. *Journal of Pharmaceutical Sciences* **1998**, *87*, 1639-1642.
14. Peeters, J.; Neeskens, P.; Tollenaere, J. P.; Remoortere, P. V.; Brewster, M. E. Characterization of the interaction of 2-hydroxypropyl-b-cyclodextrin with

- Itraconazole at pH 2, 4, and 7. *Journal of Pharmaceutical Sciences* **2002**, *91*, 1414-1422.
15. Backensfeld, T.; Muller, B. W.; Wiese, M.; Seydel, J. K. Effect of cyclodextrin derivatives on Indomethacin stability in aqueous solution. *Pharmaceutical Research* **1990**, *7*, 484-490.
 16. Pranker, R. J.; Stone, H. W.; Sloan, K. B.; Perrin, J. H. Degradation of aspartame in acidic aqueous media and its stabilization by complexation with cyclodextrins or modified cyclodextrins. *International Journal of Pharmaceutics* **1992**, *88*, 189-199.
 17. Loukas, Y. L.; Vrika, V.; Gregoriadis, G. Drugs, in cyclodextrins, in liposomes: a novel approach to the chemical stability of drugs sensitive to hydrolysis. *International Journal of Pharmaceutics* **1998**, *162*, 137-142.
 18. Dordunoo, S. K.; Burt, H. M. Solubility and stability of taxol: effects of buffers and cyclodextrins. *International Journal of Pharmaceutics* **1996**, *133*, 191-201.
 19. Frokjaer, S.; Otzen, D. E. Protein drug stability: A formulation challenge. *Nature* **2005**, *4*, 298-306.
 20. Usui, F.; Maeda, K.; Kusai, A.; Nishimura, K.; Yamamoto, K. Inhibitory effects of water-soluble polymers on precipitation of RS-8359. *International Journal of Pharmaceutics* **1997**, *154*, 59-66.
 21. Loftsson, T.; Frioriksdottir, H.; Siguroardottir, A. M.; Ueda, H. The effect of water-soluble polymers on drug-cyclodextrin complexation. *International Journal of Pharmaceutics* **1994**, *110*, 169-177.
 22. Mura, P.; Faucci, M. T.; Bettinetti, G. P. The influence of polyvinylpyrrolidone on naproxen complexation with hydroxypropyl- β -cyclodextrin. *European Journal of Pharmaceutical Sciences* **2001**, *13*, 187-194.